MDIG, a 2-oxoglutarate-dependent oxygenase, acts as an oncogene and predicts the prognosis of multiple types of cancer

FENG GENG[1], WEI YANG[2], DANDAN SONG[1], HAIJIA HOU[1], BING HAN[1], YECHENG CHEN[1] and HONGWEN ZHAO[1]

[1]Department of Pulmonary and Critical Care Medicine, The First Hospital of China Medical University; [2]Department of Pulmonary and Critical Care Medicine, General Hospital of Northern Theatre Command, Shenyang, Liaoning 110001, P.R. China

Received January 17, 2022; Accepted May 9, 2022

DOI: 10.3892/ijo.2022.5372

Abstract. Recent studies have indicated that mineral dust-induced gene (MDIG) is an oncogene induced by environmental factors, which has a key role in the development and progression of various tumor types, through epigenetic modifications; however, there are no previous pan-cancer analyses of MDIG. In the present study, a comprehensive pan-cancer analysis of MDIG was performed using public databases. The results demonstrated that MDIG was upregulated in tumor tissue samples compared with normal tissue, that it was present in all cancer cell lines and it was closely associated with the prognosis of patients with different tumor types. Furthermore, MDIG expression was closely associated with the immunological characteristics of the tumor microenvironment (TME), such as the frequency of tumor-infiltrating immune cells, TME-relevant signatures, immunostimulatory genes, immune checkpoint genes, chemokine receptor genes, tumor mutational burden and microsatellite instability. In parallel, high expression of MDIG was associated with improved overall survival of patients and this was verified in a cohort of patients who had received anti-programmed cell death 1 ligand 1 treatment. Furthermore, high expression of MDIG led to multiple drug resistance in The Cancer Genome Atlas-lung adenocarcinoma cohort. In addition, gene set variant analysis and gene set enrichment analysis indicated that MDIG was involved in cell cycle regulation. *In vitro* experiments suggested that MDIG promoted cell proliferation through the mTOR complex 2/Akt and pyruvate dehydrogenase kinase 1/Akt signaling pathways. In summary, the present study suggests that MDIG may be a prognostic biomarker and therapeutic target for various cancer types.

Correspondence to: Professor Hongwen Zhao, Department of Pulmonary and Critical Care Medicine, The First Hospital of China Medical University, 155 Nanjing Street, Heping, Shenyang, Liaoning 110001, P.R. China
E-mail: hwzhao2007@163.com

Key words: pan-cancer, mineral dust-induced gene, prognostic and therapeutic biomarker, cell proliferation, AKT signaling

Introduction

It is estimated that 19.3 million new cancer cases and nearly 10 million cancer-associated deaths occurred in 2020 worldwide (1). Furthermore, the global cancer burden is projected to reach 28.4 million cases in 2040, representing a 47% increase from 2020 (1). Cancer is largely considered a disease of gene alterations and mutations. Therefore, it is of great significance to conduct comprehensive pan-cancer studies on genes associated with the diagnosis, prognosis and treatment of cancer.

Mineral dust-induced gene (MDIG) is an oncogene that may be induced by environmental factors, including mineral dust (2), tobacco smoke (3), arsenic (4) and silica (5). It encodes a nuclear protein with a molecular weight of 53 kDa (6) and is also known as MYC induced nuclear antigen 53 (MINA53) (6), nucleolar protein 52 (7), ribosomal oxygenase 2 (RIOX2) (8) and JmjC domain-containing protein 10 (9). MDIG contributes to the occurrence and development of multiple tumors, mainly through post-translational protein hydroxylation (10) and epigenetic demethylation (via a hydroxylation reaction) (11). Previous studies have suggested that MDIG is highly expressed in a variety of tumor tissue types, including lung (12), breast (13), liver (14), colon (15) and gastric cancer (16), as well as renal cell carcinoma (17), gingival squamous cell carcinoma (18) and lymphoma (19). Furthermore, high expression of MDIG is usually associated with poor prognosis (20). Of note, another study indicated that, compared with low expression of MDIG, high expression was associated with a favorable prognosis in patients with lung cancer (21). Similarly, a study on breast cancer indicated that the expression levels of MDIG were associated with lymph node metastasis and that increased MDIG expression predicted poor overall survival (OS) in patients with lymph node metastasis (13,22,23). Furthermore, MDIG may have different roles in different stages of tumor development, promoting tumor proliferation in the early stages of tumor occurrence, but inhibiting tumor invasion and migration in the advanced stages of tumor progression (22). In addition, MDIG also has an effect on tumor therapy. A previous study by our group suggested that MDIG promoted

cisplatin resistance in lung adenocarcinoma (LUAD) by regulating ABC transporter expression via activation of the Wnt/β-catenin signaling pathway (24). Furthermore, MDIG deficiency sensitized glioblastoma cells to doxorubicin (25). In addition, MDIG induced tumor angiogenesis by promoting the activation of the EGFR/phosphorylated (P-) EGFR (Tyr1068)/VEGF-A/VEGF-R1/R2 pathway (26). In the light of these results, it may be hypothesized that MDIG is not only closely linked to cancer diagnosis and prognosis but may also affect chemotherapy and anti-angiogenic targeted therapy. It is worth noting that studies on MDIG have so far been limited to a small number of tumor types. Furthermore, studies evaluating the association between MDIG and antitumor immunity are still lacking.

The aim of the present study was to carry out a pan-cancer analysis of MDIG expression and determine its association with the prognosis and tumor microenvironment (TME)-immunological characteristics using public datasets. Furthermore, the prognostic effect of MDIG was validated in a cohort of patients with bladder carcinoma (BLCA) who had received anti-programmed cell death 1 ligand 1 (PD-L1) immunotherapy. In addition, chemotherapeutic drug sensitivity in The Cancer Genome Atlas (TCGA)-LUAD cohort was assessed and gene set variant analysis (GSVA) and gene set enrichment analysis (GSEA) were conducted in the TCGA-LUAD cohort. Finally, *in vitro* experiments were used to verify the molecular mechanisms.

Materials and methods

Analysis of MDIG expression in different types of cancer. MDIG expression in normal tissue was assessed via the Genotype-Tissue Expression (GTEx) database (https://gtexportal.org) (27) using the gene symbol RIOX2. In addition, data downloaded from the Cancer Cell Line Encyclopedia (CCLE; https://sites.broadinstitute.org/ccle/) for the gene symbol RIOX2 were used to analyze the expression of MDIG in cancer cell lines representing 30 types of cancer. Furthermore, the TCGA database (https://portal.gdc.cancer.gov/) (28), which is the largest database of cancer genetic information available, holds transcriptome data, clinical information and methylation data. The mRNA expression data from RNA-sequencing (RNA-seq) of 33 tumor types of a pan-cancer panel were downloaded for subsequent bioinformatics analysis. All data were obtained in December 2021. First, RNA-seq datasets for 33 types of cancer in TCGA were used to analyze the differences in MDIG expression between tumor and paired normal tissue samples. Next, the clinicopathological characteristics of the patients (smoking and age) were obtained from the TCGA-LUAD cohort and assessed for their association with MDIG expression. For all gene expression analyses, the RNA-seq data were downloaded as $\log_2$(TPM+1), where TPM is the transformation to transcripts per million mapped reads. Furthermore, immunohistochemical staining images of MDIG expression in normal lung and lung cancer tissue were obtained from the Human Protein Atlas (HPA; https://www.proteinatlas.org/) using the gene symbol RIOX2.

Survival analysis of MDIG in different types of cancer. The OS and progression-free interval (PFI) data of patients with different types of cancer were obtained from the University of California Santa Cruz (UCSC) Xena database (https://xena.ucsc.edu/) (29) using the gene symbol RIOX2. Univariate Cox regression (uniCox) and Kaplan-Meier (KM) analyses were performed to examine the effect of MDIG on patient survival using the R packages 'forestplot (version 1.10.1)', 'survival (version 3.210)' and 'survminer (version 0.4.9)'. The expression levels of MDIG in tumor and adjacent noncancerous tissue samples were divided into a high- and a low-expression group according to the median of the cohort.

Analysis of MDIG alterations in different types of cancer. The mutational status (alteration frequency and mutation type) of MDIG were all analyzed in TCGA tumor datasets from cBioPortal (https://www.cbioportal.org/) (30) using the 'quick selection' section to investigate 'TCGA Pan Cancer Atlas Studies'. 'RIOX2' was entered for queries regarding the genetic alteration. The 'mutations' module was used to explore the mutated site of MDIG, which is displayed in the schematic diagram of the protein structure or the three-dimensional structure. The analysis was performed and graphically presented using the 'Cancer Types Summary (version 1.20.0)' and 'Complex Heatmap (version 2.2.0)' R packages, respectively.

Promoter methylation status and the association with important oncogenes of MDIG in non-small cell lung cancer (NSCLC). Data on the promoter methylation status of MDIG in NSCLC were obtained from the UALCAN database (http://ualcan.path.uab.edu/index.html) (31) using the gene symbol MINA. The DNA methylation data were presented as β-values ranging from 0 (unmethylated) to 1 (fully methylated). Furthermore, the Spearman's correlation between the expression of MDIG and that of C-Myc, an important proto-oncogene in NSCLC (32), or tumor protein 53 (TP53), an important tumor suppressor gene in NSCLC (33), was examined in the TCGA-LUAD cohort.

Correlation analysis of MDIG expression and immunological characteristics. Cell type Identification by Estimating Relative Subsets of RNA Transcripts (CIBERSORT) (34) was used to analyze the relationship between MDIG and 22 types of tumor-infiltrating immune cell in TCGA datasets. Furthermore, the TME-relevant signatures were correlated with the immunotherapy response (35,36) and the CIBERSORT algorithm was used to quantify the content of TME-relevant signatures in different types of cancer in the CIBERSORT web portal (https://cibersort.stanford.edu) using the gene symbol RIOX2.

In addition, the relationship between the expression of MDIG and that of immune-relevant genes closely related to tumor immune escape, as well as immunotherapy responsiveness (37), were examined using the tumor-immune system interactions database (TISIDB) website (http://cis.hku.hk/TISIDB/) (38) using the gene symbol MINA. The analyzed immune-relevant genes included immunostimulatory, immune checkpoint and chemokine receptor.

Association analysis of MDIG with tumor mutational burden (TMB) and microsatellite instability (MSI). The analysis of the association between MDIG expression and TMB or MSI was performed using Spearman's correlation coefficient. The

'fmsb (version 0.7.2)', 'limma (version 3.28.14)' and 'dplyr (version 0.7.8)' R package was used to analyze the pan-cancer data of MDIG for 33 types of cancer.

Cohort validation of the prognostic value of MDIG for immunotherapy. A systemic study of immune checkpoint blockade gene expression profiles was performed. Gene expression and immunotherapeutic efficacy were obtained from the IMvigor210 cohort, which was a cohort with open information from a previous study (39), with the 'IMvigor210' package. According to the correlation between MDIG expression (RNA-seq) and patient survival, the 'surv-cutpoint' function of the 'survminer (version 0.4.9)' R package was used to divide patients into high and low MDIG expression groups according to the median of the cohort. The KM method and log-rank test were used to analyze patient OS.

Drug sensitivity analysis of MDIG in the TCGA-LUAD cohort. The response to chemotherapy for LUAD was predicted using the Genomics of Drug Sensitivity in Cancer (GDSC) database (https://www.cancerrxgene.org/) (40). The expression levels of MDIG (RNA-seq data) in the TCGA-LUAD cohort were divided into a high and a low-expression group according to the median. A total of 138 drugs had potential for the treatment of cancer. The R software package 'pRRophetic' (41) was used to predict the chemotherapy sensitivity of each sample. In brief, the half-maximal inhibitory concentration (IC_{50}) of the LUAD samples was calculated through ridge regression and the prediction accuracy was assessed by 10-fold cross-validation based on the GDSC training set (42). Furthermore, the estimated IC_{50} for each specific chemotherapeutic agent between a high- and a low-expression group was compared using the Wilcoxon's rank-sum test.

Functional enrichment analysis of MDIG in the TCGA-LUAD cohort. GSVA (43) and GSEA (44) were performed using the 'GSVA (version 1.20.0)', 'limma (version 3.28.14)' and 'clusterProfiler (version 3.16.1)' packages to identify the pathways in which the genes co-expressed with MDIG were significantly enriched in the TCGA-LUAD cohort. To determine significant gene sets in the Kyoto Encyclopedia of Genes and Genomes (KEGG) and Gene Ontology (GO) analyses, |normalized enrichment score|>1, P-value <0.05 and false discovery rate (FDR) <0.25 were used as the threshold for GSEA; pathways were considered significantly enriched when they met the sub-conditions.

Cell culture, lentiviral transduction and treatments. The human lung adenocarcinoma cell line A549 (cat. no. TCHu150) and the human umbilical vein endothelial cell line EA.hy926 (cat. no. GNHu39) were purchased from the Cell Culture Center of the Chinese Academy of Medical Sciences. The EA.hy926 cell line was originally established by fusing primary human umbilical vein cells with a thioguanine-resistant clone of A549 by exposure to polyethylene glycol. The cells were identified by short tandem repeat profiling and were free of mycoplasma infection. The cells were cultured in RPMI-1640 culture medium containing 10% fetal bovine serum (FBS; both from Hyclone; Cytiva) in a 5% CO_2 cell incubator (Thermo Fisher Scientific, Inc.) at 37˚C.

The MDIG overexpression lentiviral vector (LV-MDIG; GenBank accession no. NM_032778), empty control lentiviral vector (vector), MDIG short hairpin RNA (shRNA) silencing lentiviral vectors (shRNA1, 5'-GGGTGATTTGTTGTACTT T-3'; shRNA2, 5'-AACGATTCAGTTTCACCAA-3') and a control shRNA lentiviral vector (con, 5'-TTCTCCGAACGT GTCACGT-3') were purchased from Shanghai GeneChem Co., Ltd. The overexpression vector was sent for sequencing and designated GV365 (pUbi-MCS-3FLAG-pCMV-EGFP) and the knockdown vector was sent for sequencing and designated GV248 (phU6-MCS-PUbi-EGFP). The experimental procedures were performed according to the manufacturer's protocol. As described in a previous study by our group (26), in brief, the day before transfection, 5 ml ($5x10^4$ cells/ml) of the target cells were inoculated into a T25 flask (Corning, Inc.). When confluence reached 30-50%, the cells were incubated with lentivirus at a multiplicity of infection of 20 for A549 cells and 10 for EA.hy926 cells. The cells were maintained at 37˚C, with a 5% volume fraction of CO_2 and saturated humidity. After 72 h, stably transfected A549 cells were grown in RPMI-1640 medium supplemented with 2.0 g/ml puromycin and 10% FBS for 2 weeks. Stably transfected EA.hy926 cells were screened with 1.0 g/ml puromycin as described above.

To inhibit PI3K-dependent Akt phosphorylation and kinase activity, EA.hy926 cells transduced with LV-MDIG were treated with 30 μM LY294002 (cat. no. 9901; Cell Signaling Technology, Inc.) at 37.5˚C for 24 h.

Cell proliferation assay. For EdU assays, cells were seeded into 6-well plates at a density of $5x10^3$ cells/ml. After being subjected to the corresponding treatment, the cells were cultured for 72 h and then used for EdU assays using a commercial kit (cat. no. C0071S; Beyotime Institute of Biotechnology). The cells were incubated with 50 μM EdU solution for 12 h, fixed in 4% paraformaldehyde for 30 min at room temperature and further incubated in 5% glycine for 5 min at room temperature. The cells were washed in 1X PBS, followed by treatment with 0.5% Triton X-100 at room temperature for 30 min. The samples in each well were incubated with 100 μl Apollo® mixture (cat. no. C0071S; Beyotime Institute of Biotechnology) for 30 min at room temperature. Finally, the cell nuclei were stained using Hoechst 33342 solution (cat. no. C0071S-6; Beyotime Institute of Biotechnology) at 25˚C for 25 min. Images were captured using a fluorescence microscope (Observer A1; ZEISS). The number of EdU-positive cells was counted using ImageJ software (version 1.8.0_172; National Institutes of Health).

For Cell Counting Kit-8 (CCK-8) assays, transfected A549 and EA.hy926 cells were seeded at a density of $5x10^3$ cells/well and were examined at 6, 24, 48, 72 and 96 h post-transfection according to the manufacturer's protocols. Cell viability was evaluated using a CCK-8 kit (Beyotime Institute of Biotechnology). In brief, CCK-8 solution was added to each well and the cells were incubated for an additional 2 h. The absorbance at 450 nm was measured using a microplate reader (Tecan Infinite M200PRO; Tecan Group, Ltd.).

Western blot analysis. Cells were lysed using lysis buffer (cat. no. 9803S; Cell Signaling Technology, Inc.) supplemented with a protease inhibitor cocktail (cat. no. 11697498001; Roche

Diagnostics GmbH) for 30 min at 4˚C. The protein concentration was measured by a bicinchoninic acid assay (Thermo Fisher Scientific, Inc.). A total of 30 μg protein per lane was separated using 8-14% SDS-PAGE (Bio-Rad Laboratories, Inc.) and transferred to PVDF membranes (Merck Life Sciences, Inc.), which were then blocked at room temperature for 2 h with 5% skimmed dried milk (cat. no. 1172GR500; BioFroxx). The membranes were subsequently washed with 1X Tris-buffered saline containing 0.1% Tween®-20 detergent (1X TBST) and then incubated with primary antibodies against MINA53 (cat. no. sc-398521), cyclin-dependent kinase (CDK)2 (cat. no. sc-6248), CDK6 (cat. no. sc-7961), CDK inhibitor 1A (CDKN1A; cat. no. sc-6246), CDKN2D (cat. no. sc-1665; all at 1:1,000 dilution; mouse monoclonal; Santa Cruz Biotechnology, Inc.), pan-Akt (cat. no. 4691), pyruvate dehydrogenase kinase 1 (PDK1; cat. no. 13037), P-PDK1 (Ser241; cat. no. 3438), P-Akt (Thr308; cat. no. 13038), mTOR (cat. no. 2983), GβL (cat. no. 3274), Rictor (cat. no. 9476), P-Akt (Ser473; cat. no. 4060) and GAPDH (cat. no. 5174; all at 1:1,000 dilution; rabbit monoclonal; Cell Signaling Technology, Inc.) at 4˚C overnight. After another wash with 1X TBST, the membranes were incubated with anti-mouse IgG (cat. no. sc-2005; 1:3,000 dilution; Santa Cruz Biotechnology, Inc.) or anti-rabbit IgG (cat. no. 7074; 1:3,000 dilution; Cell Signaling Technology, Inc.) as the secondary antibody at room temperature for 2 h. Immunoreactive bands were detected using an enhanced chemiluminescence (ECL) western blotting system (Clarity Western ECL Substrate; Bio-Rad Laboratories, Inc.). The greyscale densities of the bands were measured using Image J software (version 1.8.0_172; National Institutes of Health), and the density ratio of each protein band was normalized to that of GAPDH and expressed as the percentage of the corresponding control group. Phosphoproteins were presented as the ratio of phosphoprotein to total protein.

Statistical analysis. All statistical analyses were performed using R (version 4.0.3) and R packages 'ggplot2 (version 3.3.3)', 'ggpubr (version 0.4.0)', 'pheatmap (version 1.0.12)' and 'cowplot (version 1.1.1)' were used for visualization. In the bioinformatics analyses, Kruskal-Wallis tests were performed to examine the differences in MDIG expression between different tissue types and cancer cell lines. Furthermore, Kruskal-Wallis tests were performed to examine the differences in the clinicopathological characteristics of the patients (smoking and age), followed by Dunn's test. The significance of the difference in gene expression between cancerous and para-cancerous normal tissues, the drug sensitivity analysis, and the correlation analysis between MDIG expression and TME-relevant signatures in BLCA were determined using Wilcoxon's rank-sum test. Patient prognosis was evaluated using uniCox and the results were presented as the hazard ratio (HR) with 95% confidence interval and P-values. The KM method with log-rank tests was used to estimate the survival probability against time, but when there was a late-stage crossover between the groups, Renyi-type tests were used, with the results presented as P-values. The correlation between MDIG expression and immunological characteristics was evaluated using Pearson's correlation or Spearman's correlation tests. P<0.05 was considered to indicate a statistically significant difference.

All data obtained from *in vitro* experiments were expressed as the mean ± standard deviation. Comparisons between groups were performed using one-way ANOVA (CCK-8 assay, EdU assay and western blotting) followed by Tukey's post-hoc test by RStudio (RStudio; https://www.rstudio.com). P<0.05 was considered to indicate a statistically significant difference. All experiments were performed at least three times.

Results

Expression of MDIG in different types of cancer. In the datasets obtained from the GTEx database, MDIG was significantly differentially expressed in all human tissues and organs, among which the thyroid gland and skeletal muscle had high expression levels, while the testis and lung had low expression levels (Fig. 1A). Furthermore, the expression levels of MDIG in 1,363 cell lines from 30 types of cancer were analyzed in CCLE datasets. The results indicated that MDIG was significantly differentially expressed in most cancer cell lines compared to each other (Fig. 1B).

MDIG expression in cancer and paired adjacent tissue samples was then analyzed in TCGA datasets. MDIG was significantly upregulated in BLCA, cholangiocarcinoma (CHOL), colon adenocarcinoma (COAD), esophageal carcinoma (ESCA), glioblastoma (GBM), liver hepatocellular carcinoma (LIHC), LUAD, lung squamous cell carcinoma (LUSC), prostate adenocarcinoma (PRAD), rectum adenocarcinoma (READ) and stomach adenocarcinoma (STAD) tumor tissue compared with normal adjacent tissue. By contrast, MDIG expression was significantly downregulated in breast invasive carcinoma (BRCA), kidney renal clear cell carcinoma (KIRC), kidney renal papillary cell carcinoma (KIRP) and thyroid carcinoma (THCA) (Fig. 1C). At the protein level, immunohistochemistry images from the HPA suggested that MDIG protein was expressed at low levels in normal lung tissue but markedly upregulated in lung cancer tissue (Fig. 2A). In addition, MDIG expression was significantly higher in patients with LUAD and a history of smoking than in those without a history of smoking. Furthermore, MDIG expression levels were significantly lower after smoking cessation but did not change with the duration of cessation (Fig. 2B). However, age did not affect MDIG expression in LUAD (Fig. 2C).

Survival analysis of MDIG in different types of cancer. Since MDIG was highly expressed in several types of tumor tissue, the UCSC Xena database was used to examine the association between MDIG and clinical prognosis in different types of cancer. The uniCox OS results indicated that MDIG was a risk factor in KIRP (HR=1.352, P=0.002), brain lower grade glioma (LGG) (HR=1.224, P<0.001), LIHC (HR=1.154, P<0.001), pancreatic adenocarcinoma (PAAD) (HR=1.332, P=0.022), PRAD (HR=1.458, P=0.028) and sarcoma (SARC) (HR=1.157, P=0.010). Of note, the opposite results were found for READ (HR=0.549, P=0.001) and uveal melanoma (UVM) (HR=0.596, P=0.039) (Fig. 3). For the PFI, MDIG was a risk factor in BLCA (HR=1.112, P=0.005), KIRP (HR=1.244, P=0.019), LGG (HR=1.202, P<0.001), LIHC (HR=1.097, P=0.009), PAAD (HR=1.304, P=0.026) and uterine corpus endometrial carcinoma (UCEC) (HR=1.172, P=0.006). However, the opposite result was obtained for

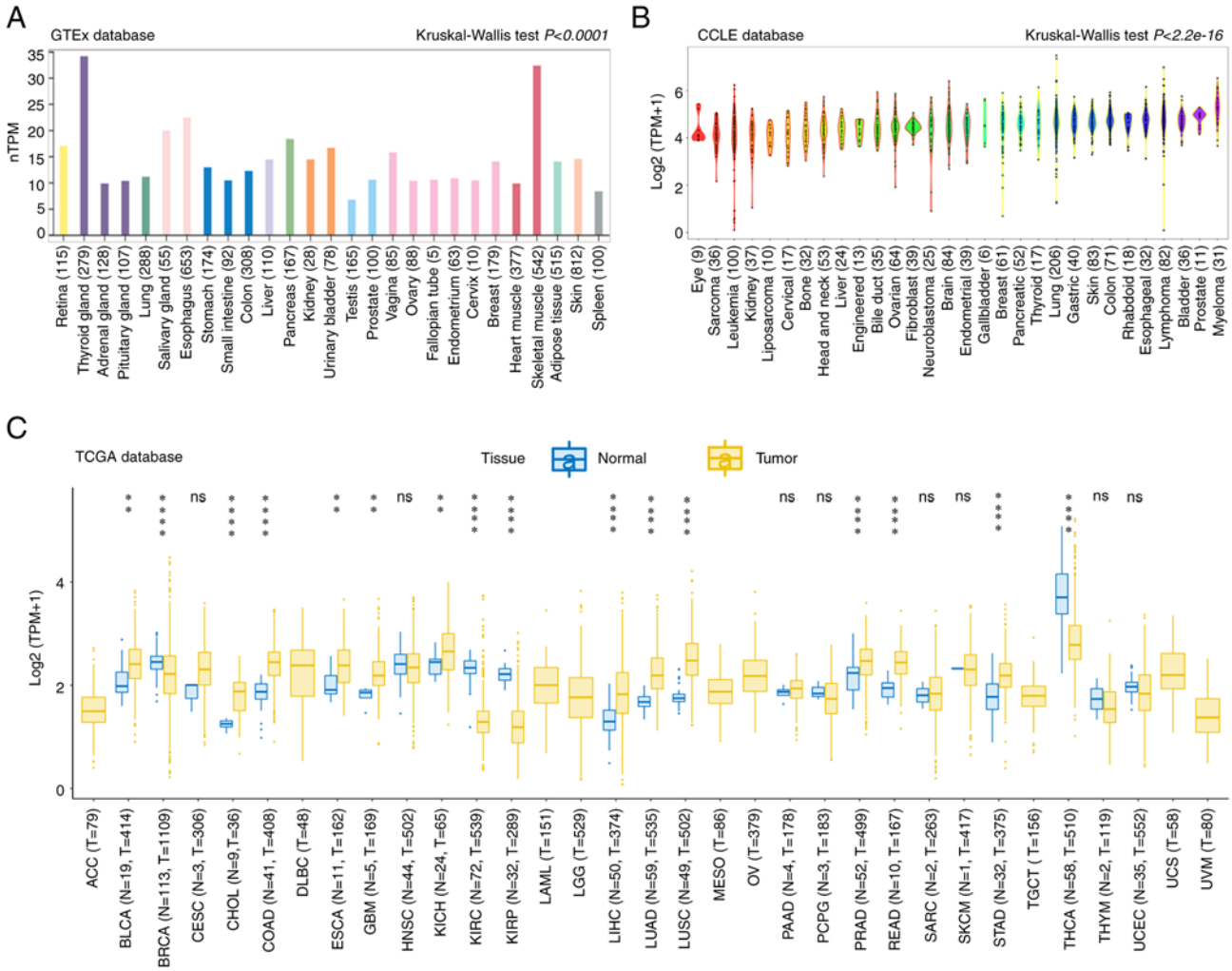

Figure 1. MDIG expression in various types of cancer. (A) Different expression levels of MDIG among 27 normal tissue types in a GTEx dataset determined using Kruskal-Wallis tests. (B) Different expression levels of MDIG among cancer cell lines representing 30 types of cancer in a CCLE dataset according to Kruskal-Wallis tests. (C) Expression levels of MDIG in a dataset from TCGA comprising 33 tumor tissue types and paired adjacent noncancerous tissue (Wilcoxon rank-sum test). Data in the box plot are presented as the median and 25-75th percentile, and the vertical bars indicate the standard deviation and the dots outliers. **P<0.01, ****P<0.0001. ns, no significance; N, normal; T, tumor; MDIG, mineral dust-induced gene; TPM, transcripts per million mapped reads; GTEx, Genotype-Tissue Expression; CCLE, Cancer Cell Line Encyclopedia; TCGA, The Cancer Genome Atlas; ACC, adrenocortical carcinoma; BLCA, bladder urothelial carcinoma; BRCA, breast invasive carcinoma; CESC, cervical squamous cell carcinoma; CHOL, cholangiocarcinoma; COAD, colon adenocarcinoma; DLBC, diffuse large B cell lymphoma; ESCA, esophageal carcinoma; GBM, glioblastoma; HNSC, head and neck squamous cell carcinoma; KICH, kidney chromophobe; KIRC, kidney renal clear cell carcinoma; KIRP, kidney renal papillary cell carcinoma; LAML, acute myeloid leukemia; LGG, brain lower grade glioma; LIHC, liver hepatocellular carcinoma; LUAD, lung adenocarcinoma; LUSC, lung squamous cell carcinoma; MESO, mesothelioma; OV, ovarian serous cystadenocarcinoma; PAAD, pancreatic adenocarcinoma; PCPG, pheochromocytoma and paraganglioma; PRAD, prostate adenocarcinoma; READ, rectum adenocarcinoma; SARC, sarcoma; SKCM, skin cutaneous melanoma; STAD, stomach adenocarcinoma; TGCT, testicular germ cell tumors; THCA, thyroid carcinoma; THYM, thymoma; UCEC, uterine corpus endometrial carcinoma; UCS, uterine carcinosarcoma; UVM, uveal melanoma.

pheochromocytoma and paraganglioma (HR=0.581, P=0.031) (Fig. 3).

In addition, in the KM analysis of OS, high MDIG expression predicted unfavorable OS in patients with BRCA, KIRP, LGG, LIHC, PAAD, SRAC and UCEC (Fig. 4). Furthermore, high MDIG expression predicted shorter PFI times in patients with KIRP, LGG, LIHC, PAAD and UCEC (Fig. 4).

Gene alteration analysis of MDIG in different types of cancer. The highest alteration frequency of MDIG (~8%) was observed in patients with LUSC. 'Amplification' was the primary type for LUSC, cervical squamous cell carcinoma and head and neck squamous cell carcinoma, with an alteration frequency of ~7, ~4 and ~3%, respectively (Fig. 5A). However, MDIG mutations were not prevalent in any other types of cancer tissue (Fig. 5A). There was no significant association between MDIG mutations and patient prognosis (data not shown).

Promoter methylation status and the association between MDIG, C-Myc and TP53 expression in LUAD. As presented in Fig. 5B, the promoter methylation levels of MDIG in LUSC and LUAD were significantly lower than those in normal lung tissue from TCGA data. In addition, MDIG expression was significantly positively correlated with that of C-Myc in LUAD (stages II/III). The correlation gradually increased from stage I to stage III, then decreased at stage IV and was no longer statistically significant. Of note, the significance became stronger with increasing stage was observed for the

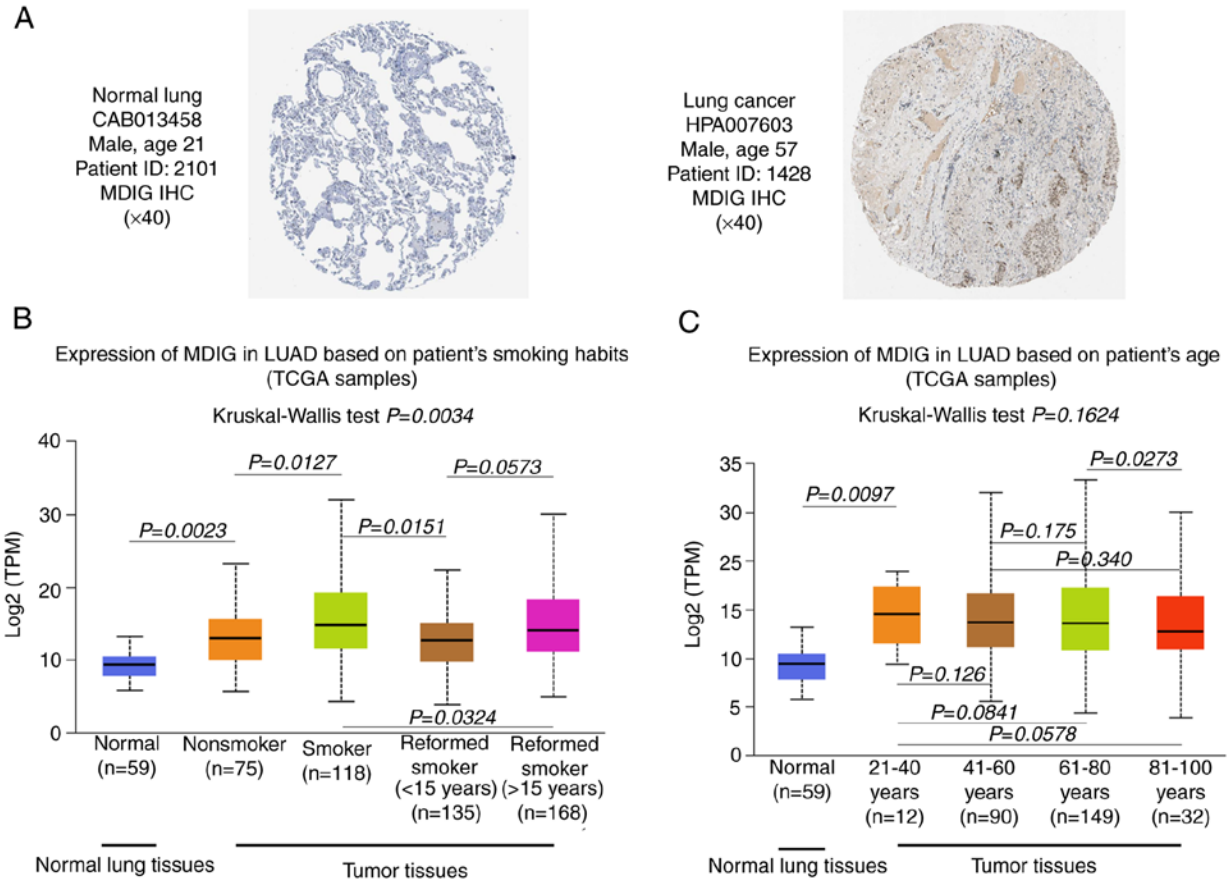

Figure 2. MDIG expression in lung cancer. (A) MDIG expression in normal lung and lung cancer tissue samples from the Human Protein Atlas (magnification, x40). (B) MDIG expression in patients with LUAD from TCGA data stratified according to their smoking history (Kruskal-Wallis tests followed by Dunn's tests). (C) MDIG expression in patients with LUAD from TCGA data stratified according to their age (Kruskal-Wallis tests followed by Dunn's tests). MDIG, mineral dust-induced gene; LUAD, lung adenocarcinoma; TCGA, The Cancer Genome Atlas; IHC, immunohistochemistry; TPM, transcripts per million mapped reads.

correlation analysis between MDIG and TP53 expression (Fig. 5C).

Correlation of MDIG expression with immunological characteristics. In most types of cancer, MDIG expression positively correlated with the frequency of 'Macrophages M1', 'T cells CD4$^+$ memory activated', and 'T cells CD4$^+$ memory resting'. However, MDIG expression significantly negatively correlated with 'T cells CD8$^+$', 'NK cells activated' and 'T cells regulatory (Tregs)' (Fig. 6A). As indicated in Fig. 6B, MDIG expression positively correlated with TME-relevant signatures (such as 'Nucleotide_excision_repair', 'Mismatch_Repair', 'DNA_replication' and 'DNA_damage_response'). However, MDIG expression had a significant negative correlation with TME-relevant signatures in KIRC and THCA.

Association of MDIG with immune-relevant genes, TMB and MSI. MDIG expression correlated with that of several immune-relevant genes, albeit with different patterns in different tumor types. MDIG was positively correlated with immunostimulatory genes in most types of cancer, such as LIHC, CHOL, BLCA, thymoma (THYM) and LUAD. However, there was a negative correlation between KIRC and THCA (Fig. 7A). As presented in Fig. 7D, MDIG was significantly associated with immune checkpoint genes in most types of tumor. Furthermore, there was a significant positive correlation between MDIG and PD-L1 in most types of tumor. Of note, MDIG was negatively correlated with immune checkpoint genes in KIRC and THCA. In addition, MDIG was significantly positively correlated with chemokine receptor genes in BLCA, PAAD, CHOL and diffuse large B cell lymphoma (DLBC), amongst others, but significantly negatively correlated with chemokine receptor genes in KIRC and THCA (Fig. 7E). Overall, there was a close correlation between immune-relevant genes and MDIG and MDIG was always significantly negatively correlated with immune-relevant genes in KIRC and THCA.

TMB (45) and MSI (46) are important molecular markers for immune checkpoint block therapy. MDIG expression positively correlated with TMB in LUAD, BLCA, STAD and UCEC, but negatively correlated in KIRC and THCA (Fig. 7B). As presented in Fig. 7C, MDIG also positively correlated with MSI in STAD, THYM and LUSC. However, the opposite results were observed in DLBC, THCA and skin cutaneous melanoma.

Cohort validation of the prognostic role of MDIG for immunotherapy. The effect of MDIG on TME-relevant signatures in BLCA was analyzed using the CIBERSORT algorithm. The results suggested that high expression of MDIG

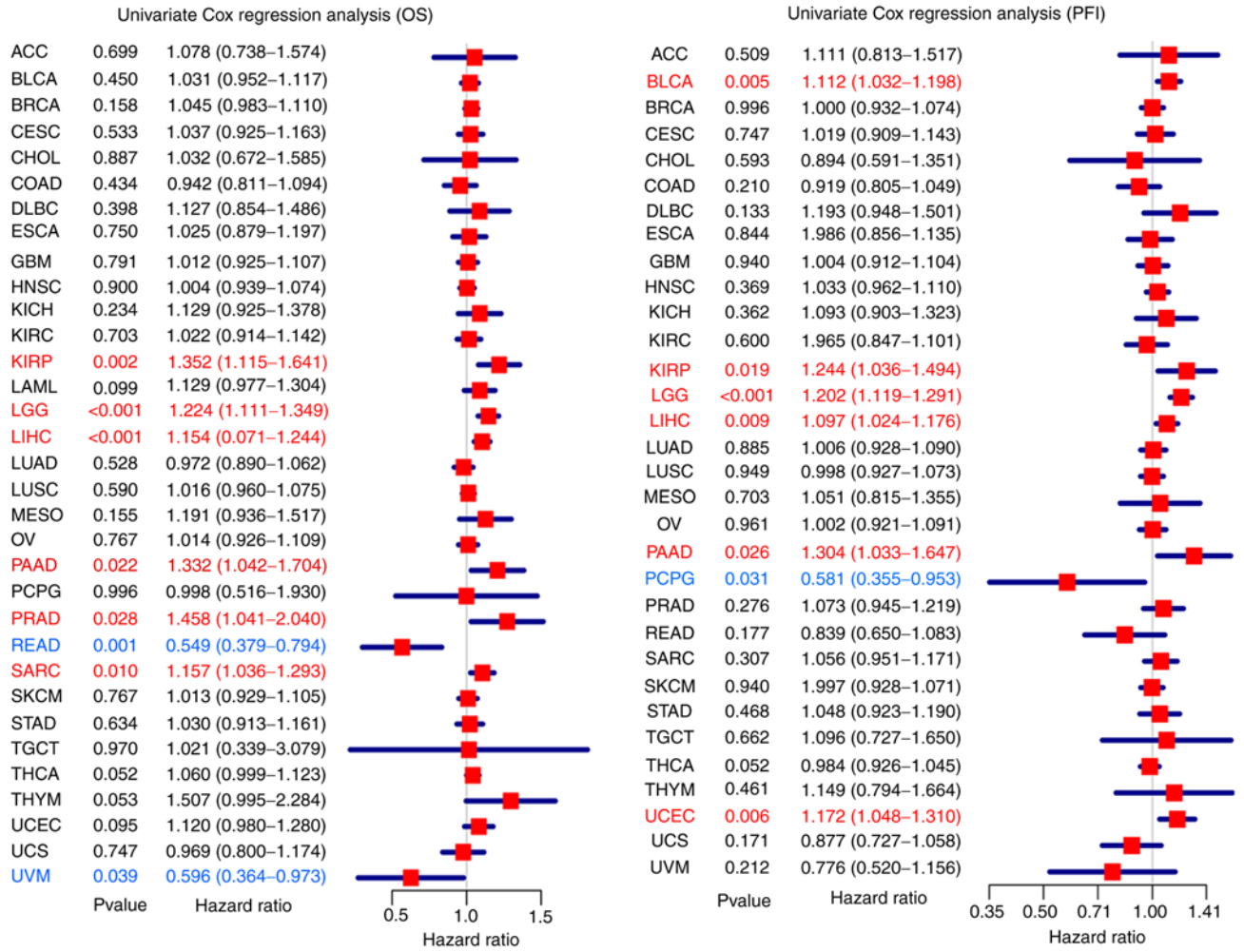

Figure 3. Relationship between high expression of MDIG and patient OS (left panel) and PFI (right panel). The forest plots were generated using univariate survival analysis in various cancer types. HR>1 indicates that MDIG high expression represents a risk factor, whereas HR<1 suggests that it is a protective factor. MDIG, mineral dust-induced gene; HR, hazard ratio; OS, overall survival; PFI, progression-free interval; ACC, adrenocortical carcinoma; BLCA, bladder urothelial carcinoma; BRCA, breast invasive carcinoma; CESC, cervical squamous cell carcinoma; CHOL, cholangiocarcinoma; COAD, colon adenocarcinoma; DLBC, diffuse large B cell lymphoma; ESCA, esophageal carcinoma; GBM, glioblastoma; HNSC, head and neck squamous cell carcinoma; KICH, kidney chromophobe; KIRC, kidney renal clear cell carcinoma; KIRP, kidney renal papillary cell carcinoma; LAML, acute myeloid leukemia; LGG, brain lower grade glioma; LIHC, liver hepatocellular carcinoma; LUAD, lung adenocarcinoma; LUSC, lung squamous cell carcinoma; MESO, mesothelioma; OV, ovarian serous cystadenocarcinoma; PAAD, pancreatic adenocarcinoma; PCPG, pheochromocytoma and paraganglioma; PRAD, prostate adenocarcinoma; READ, rectum adenocarcinoma; SARC, sarcoma; SKCM, skin cutaneous melanoma; STAD, stomach adenocarcinoma; TGCT, testicular germ cell tumors; THCA, thyroid carcinoma; THYM, thymoma; UCEC, uterine corpus endometrial carcinoma; UCS, uterine carcinosarcoma; UVM, uveal melanoma.

was associated with 'CD-8-T-effector', 'Immune-Checkpoint', 'Antigen-processing-machinery', 'TMEscoreA', 'Mismatch-Repair', 'Nucleotide-excision-repair', 'pan tissue fibroblast TGF-β response signature (Pan-F-TBRs)', 'epithelial-to-mesenchymal transition (EMT)1/2/3' and 'TMEscoreB' (Fig. 8A). Furthermore, KM analysis of OS indicated that MDIG high expression was associated with favorable OS in patients with BLCA who had received PD-L1 immunotherapy (Fig. 8B).

Drug sensitivity analysis of MDIG in TCGA-LUAD cohort. While several treatment options are available for lung cancer at present, chemotherapy remains widely used (47). The GDSC database was used to analyze the relationship between MDIG expression and sensitivity to chemotherapeutic drugs in the TCGA-LUAD cohort. As presented in Fig. 9, for AKT.inhibitor.VIII, cisplatin, CCT018159, CGP.082996, gemcitabine and camptothecin, the estimated IC_{50} was higher with high expression of MDIG as compared with the low-expression group.

Functional enrichment analysis of MDIG in LUAD. To obtain deeper insight into the biological functions associated with MDIG, GSVA and GSEA were used to identify pathways enriched by MDIG. As presented in Fig. 10A, the results of the GSVA indicated that the pathways in which the genes co-expressed with MDIG were enriched were G2M-CHECKPOINT, E2F-TARGETS, UNFOLDED-PROTEIN-RESPONSE, MTORC1-SIGNALING, MYC-TARGETS-V1/2, SPERMATOGENESIS, MITOTIC-SPINDLE, GLYCOLYSIS and PI3K-AKT-MTOR-SIGNALING. Furthermore, GSEA-GO and GSEA-KEGG were performed to identify enriched GO terms in the category biological process (GOBP) and KEGG pathways in association with MDIG in LUAD. The results

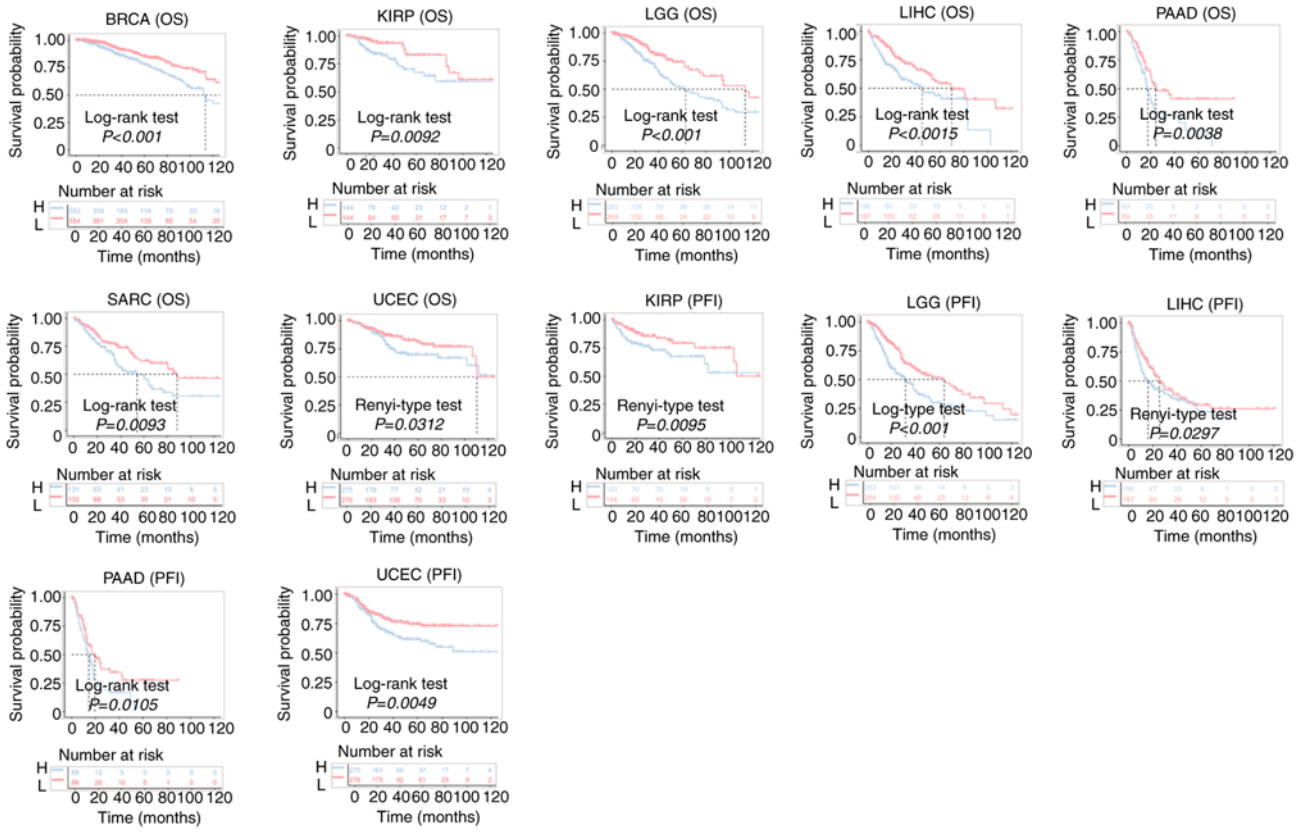

Figure 4. Kaplan-Meier curves for OS and PFI of patients from TCGA datasets stratified according to MDIG gene expression. MDIG, mineral dust-induced gene; OS, overall survival; PFI, progression-free interval; H, high expression; L, low expression; BRCA, breast invasive carcinoma; KIRP, kidney renal papillary cell carcinoma; LGG, brain lower grade glioma; LIHC, liver hepatocellular carcinoma; PAAD, pancreatic adenocarcinoma; SARC, sarcoma; UCEC, uterine corpus endometrial carcinoma.

suggested that the genes co-expressed with MDIG were enriched in biological process terms and pathways such as GOBP-CELL-G1-S-PHASE-TRANSITION, GOBP-CELL-DIVISION, GOBP-COVALENT-CHROMATIN-MODIFICATION, GOBP-DNA-CONFORMATION-CHANGE, GOBP-DNA-REPAIR, KEGG-ARACHIDONIC-ACID-METABOLISM, KEGG-ASTHMA, KEGG-AUTOIMMUNE-THYROID-DISEASE, KEGG-CARDIAC-MUSCLE-CONTRACTION and KEGG-CELL-CYCLE (Fig. 10B).

MDIG promotes cell proliferation through the Akt signaling pathway in vitro. The results suggested that MDIG was upregulated in lung cancer cell lines and enrichment analysis suggested that the main biological processes of MDIG were related to the cell cycle and Akt signaling. To our knowledge, there have been no previous studies indicating that MDIG may promote cell proliferation through the Akt signaling pathway; the Akt signaling pathway is one of the most important signaling pathways that promote cell proliferation (48). Therefore, the A549 cell line (with high expression of MDIG; this cell line was thus used for MDIG knockdown studies) and the EA.hy926 cell line (which lacks MDIG expression and was thus used for MDIG overexpression studies; this cell line may be more comparable to A549 cells than other cell lines in terms of cell source) were selected for *in vitro* experiments to verify that MDIG promotes cell proliferation through the Akt signaling pathway. EdU and CCK-8 assays suggested that MDIG silencing significantly inhibited A549 cell proliferation, whereas overexpression of MDIG significantly promoted the proliferation of EA.hy926 cells. Furthermore, the addition of PI3K/Akt inhibitor (LY294002) to MDIG-overexpressing EA.hy926 cells significantly inhibited cell proliferation (Fig. 11).

Furthermore, western blot analysis was performed on MDIG-knockdown A549 cells and MDIG-overexpressing EA.hy926 cells to examine the role of Akt signaling and its downstream regulation of cell cycle-related proteins. In MDIG-knockdown A549 cells, the levels of P-PDK1 (Ser241), P-Akt (Thr308), GβL, Rictor, P-Akt (Ser473), CDK2 and CDK6 were significantly reduced (Figs. 12 and 13), whereas the expression levels of CDKN1A and CDKN2D were significantly increased compared with those in the control group (Fig. 13). However, the expression levels of Akt (pan), PDK1 and mTOR were not significantly altered (P>0.05; Fig. 12). The opposite effects were obtained for MDIG-overexpressing EA.hy926 cells (Figs. 12 and 13). As indicated in Fig. 13, in EA.hy926 cells, when comparing the LV-MDIG + LY294002 group with the LV-MDIG group, the effects of LV-MDIG on the expression levels of P-Akt (Thr308), CDK2, CDK6 and CDKN1A were reversed by LY294002, but those of CDKN2D were not. These results suggested that MDIG promoted the phosphorylation of PDK1 (Ser241) and the expression of GβL and Rictor. This may promote the phosphorylation of Akt

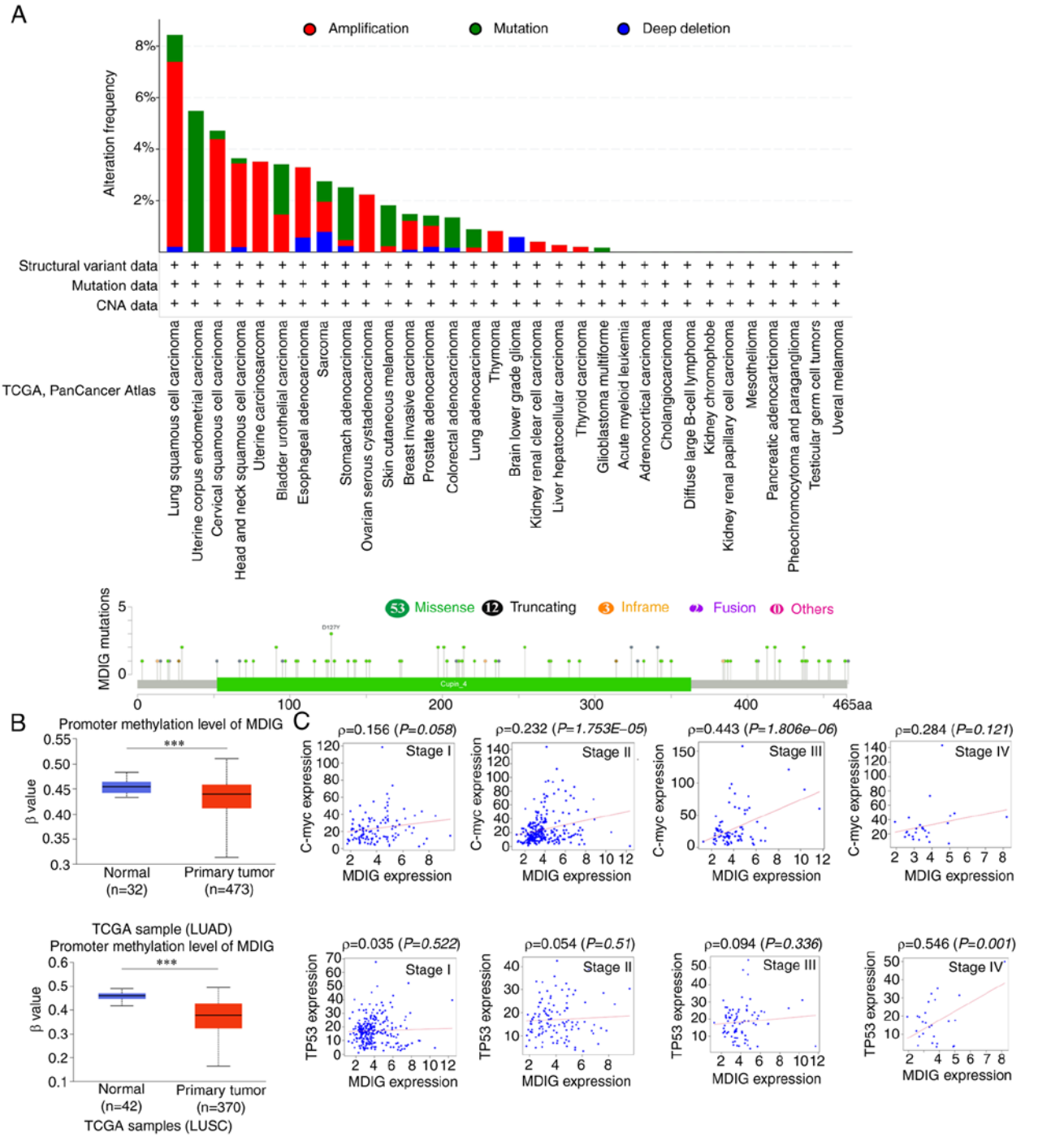

Figure 5. MDIG mutations and promoter methylation status in various cancer types and association of MDIG with C-Myc and TP53 expression in NSCLC. (A) Alteration frequency and mutation count in the MDIG gene in TCGA datasets obtained through the cBioPortal database. (B) MDIG promoter methylation status in NSCLC datasets obtained from the UALCAN database. (C) Relationship between MDIG expression and C-Myc and TP53 in TCGA datasets. ***P<0.001. MDIG, mineral dust-induced gene; NSCLC, non-small cell lung cancer; TCGA, The Cancer Genome Atlas; LUAD, lung adenocarcinoma; LUSC, lung squamous carcinoma; ρ, Spearman's correlation coefficient; TP53, tumor protein 53; CNA, copy number alteration.

(Thr308) and Akt (Ser473), leading to an increase in CDK2 and CDK6 and a decrease in CDKN1A and CDKN2D, which may in turn promote cell proliferation.

Discussion

MDIG is a member of the Jumonji-C domain-containing protein family. Evidence suggests that the MDIG protein is mainly expressed in the nucleus, diffused uniformly in the nucleoplasm and absent from the cytoplasm, but highly enriched in the nuclear and nucleolar fractions (7). Furthermore, a previous study indicated that MDIG promotes gene expression through the demethylation of histones H3K9me3, H3K27me3 and H4K20me3, thus modulating the behavior of a variety of tumors (11).

While previous clinical studies with small samples were limited to a small number of cancer types and had certain contradictory findings, the present pan-cancer analysis

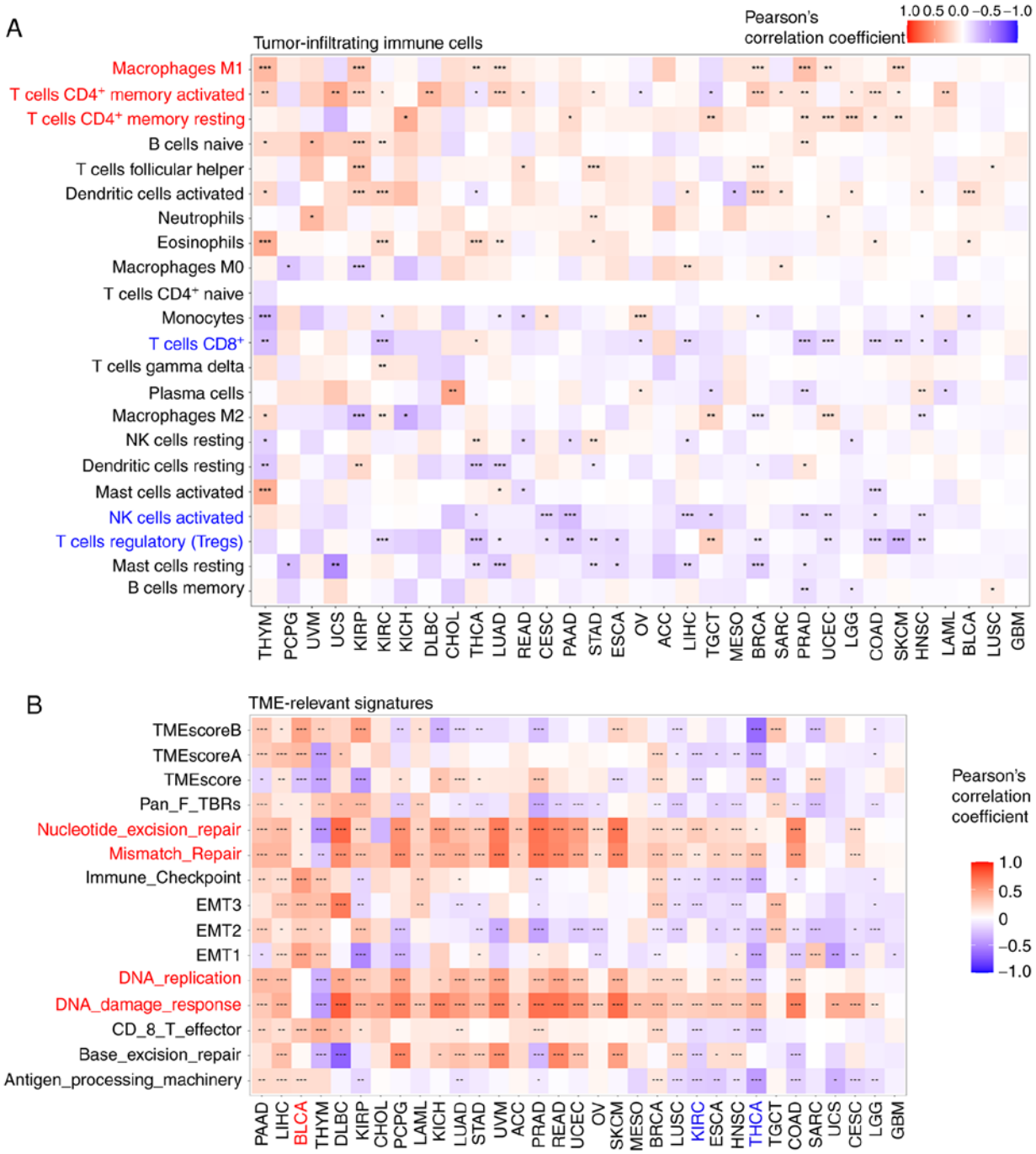

Figure 6. Correlation analysis between MDIG expression and the frequency of tumor-infiltrating immune cells and TME-relevant signatures in various cancer types. (A) Correlation analysis between MDIG expression and the frequency of tumor-infiltrating immune cells. (B) Correlation analysis between MDIG expression and TME-relevant signatures obtained through the CIBERSORT web portal. *P<0.05, **P<0.01, ***P<0.001. MDIG, mineral dust-induced gene; TME, tumor microenvironment; CIBERSORT, Cell type Identification by Estimating Relative Subsets of RNA Transcripts; EMT, epithelial-to-mesenchymal transition; Pan-F-TBR, pan tissue fibroblast TGF-β response signature; NK, natureal killer; ACC, adrenocortical carcinoma; BLCA, bladder urothelial carcinoma; BRCA, breast invasive carcinoma; CESC, cervical squamous cell carcinoma; CHOL, cholangiocarcinoma; COAD, colon adenocarcinoma; DLBC, diffuse large B cell lymphoma; ESCA, esophageal carcinoma; GBM, glioblastoma; HNSC, head and neck squamous cell carcinoma; KICH, kidney chromophobe; KIRC, kidney renal clear cell carcinoma; KIRP, kidney renal papillary cell carcinoma; LAML, acute myeloid leukemia; LGG, brain lower grade glioma; LIHC, liver hepatocellular carcinoma; LUAD, lung adenocarcinoma; LUSC, lung squamous cell carcinoma; MESO, mesothelioma; OV, ovarian serous cystadenocarcinoma; PAAD, pancreatic adenocarcinoma; PCPG, pheochromocytoma and paraganglioma; PRAD, prostate adenocarcinoma; READ, rectum adenocarcinoma; SARC, sarcoma; SKCM, skin cutaneous melanoma; STAD, stomach adenocarcinoma; TGCT, testicular germ cell tumors; THCA, thyroid carcinoma; THYM, thymoma; UCEC, uterine corpus endometrial carcinoma; UCS, uterine carcinosarcoma; UVM, uveal melanoma.

comprehensively revealed the expression, prognosis and gene function of MDIG in all common tumor types using large samples with comprehensive information from public databases. MDIG was expressed at low levels in almost all normal human tissue types. These results suggested that MDIG may have an important role in embryonic development or basic physiological activities of cells. Of note, a previous study indicated that MDIG was essential for normal

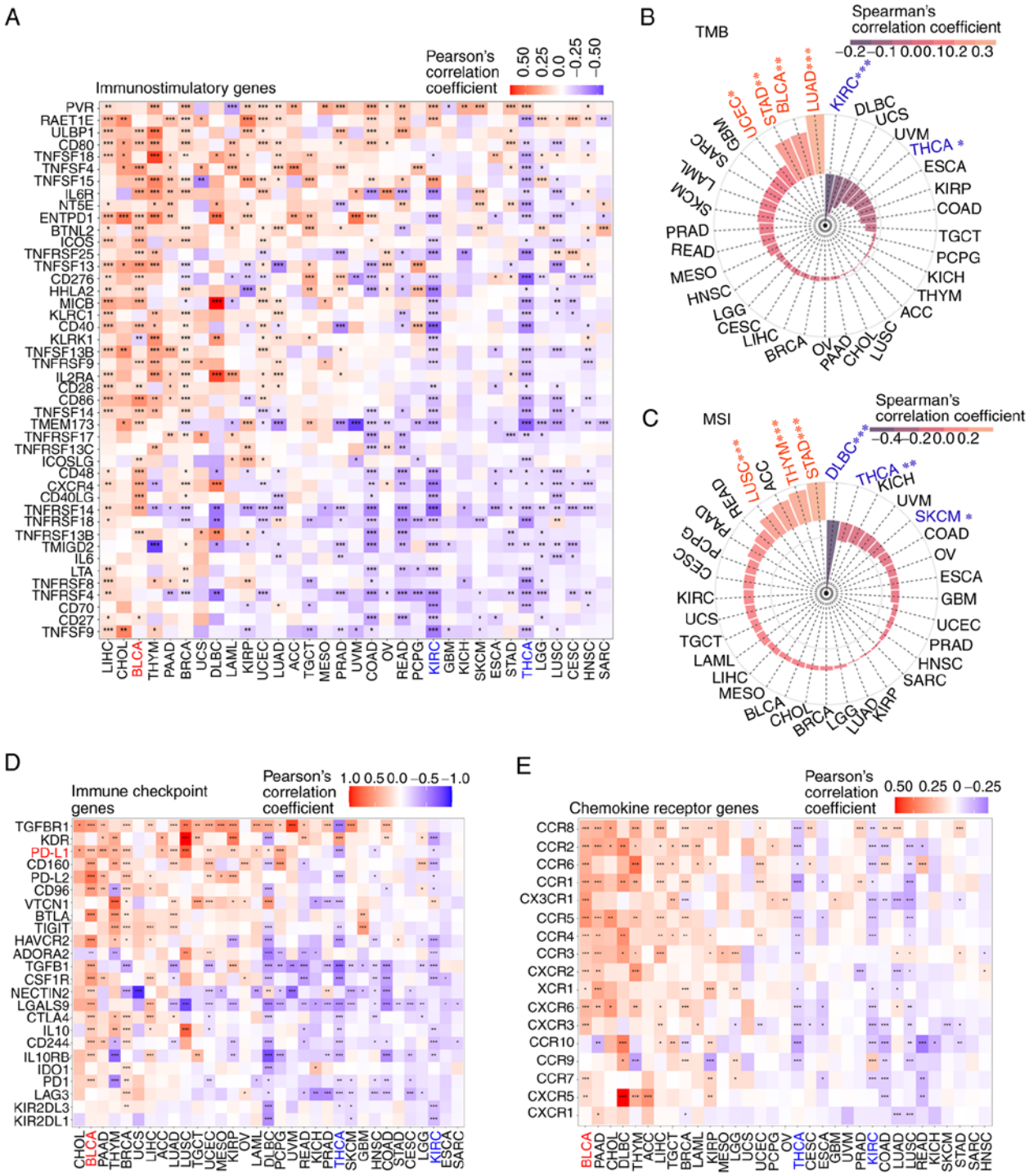

Figure 7. Analysis of the correlation of MDIG with immune-relevant genes, TMB and MSI. (A) Correlation analysis between MDIG expression and immunostimulatory genes. (B) Correlation between MDIG expression and TMB. (C) Correlation between MDIG expression and MSI. (D) Correlation analysis between MDIG expression and immune checkpoint genes. (E) Correlation analysis between MDIG expression and chemokine receptor genes. *P<0.05, **P<0.01, ***P<0.001. MDIG, mineral dust-induced gene; TMB, tumor mutational burden; MSI, microsatellite instability; ACC, adrenocortical carcinoma; BLCA, bladder urothelial carcinoma; BRCA, breast invasive carcinoma; CESC, cervical squamous cell carcinoma; CHOL, cholangiocarcinoma; COAD, colon adenocarcinoma; DLBC, diffuse large B cell lymphoma; ESCA, esophageal carcinoma; GBM, glioblastoma; HNSC, head and neck squamous cell carcinoma; KICH, kidney chromophobe; KIRC, kidney renal clear cell carcinoma; KIRP, kidney renal papillary cell carcinoma; LAML, acute myeloid leukemia; LGG, brain lower grade glioma; LIHC, liver hepatocellular carcinoma; LUAD, lung adenocarcinoma; LUSC, lung squamous cell carcinoma; MESO, mesothelioma; OV, ovarian serous cystadenocarcinoma; PAAD, pancreatic adenocarcinoma; PCPG, pheochromocytoma and paraganglioma; PRAD, prostate adenocarcinoma; READ, rectum adenocarcinoma; SARC, sarcoma; SKCM, skin cutaneous melanoma; STAD, stomach adenocarcinoma; TGCT, testicular germ cell tumors; THCA, thyroid carcinoma; THYM, thymoma; UCEC, uterine corpus endometrial carcinoma; UCS, uterine carcinosarcoma; UVM, uveal melanoma.

embryogenesis (5); in that study, the researchers were able to obtain MDIG heterozygotic knockout (MDIG$^{+/-}$) mice, but not the homozygotic mice, indicating that *MDIG* is essential for normal embryogenesis and was involved in ribosome formation by catalyzing (2S,3S)-3-hydroxyhistidine modification of Rpl27a at residue 39 (10). Similarly, in the present enrichment

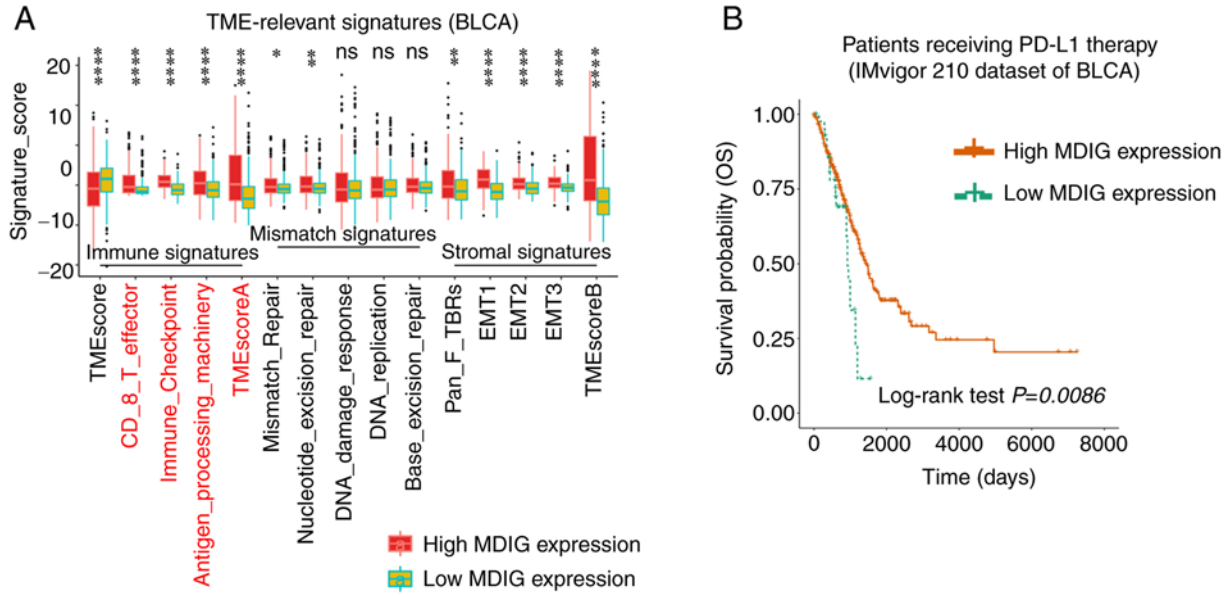

Figure 8. Association of MDIG with TME-relevant signatures and immune checkpoint blockade therapy in BLCA. (A) Correlation analysis between MDIG expression and TME-relevant signatures in BLCA obtained through the CIBERSORT web portal (Wilcoxon rank-sum test). (B) Kaplan-Meier curve analysis of OS in patients who had received anti-PD-L1 immunotherapy, stratified according to MDIG expression. *P<0.05, **P<0.01, ****P<0.0001. BLCA, bladder urothelial carcinoma; TME, tumor microenvironment; EMT, epithelial-to-mesenchymal transition; Pan-F-TBR, pan tissue fibroblast TGF-β response signature; OS, overall survival; CIBERSORT, Cell type Identification by Estimating Relative Subsets of RNA Transcripts; PD-L1, programmed cell death 1 ligand 1.

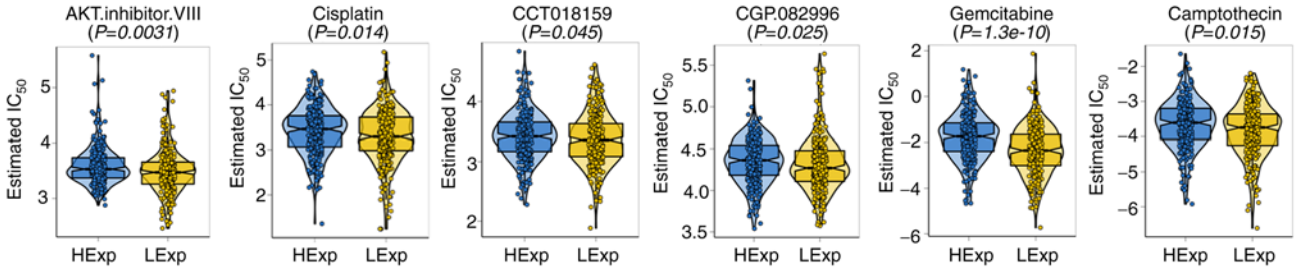

Figure 9. Relationship between MDIG expression and drug sensitivity in TCGA-LUAD cohort (Wilcoxon rank-sum test). The boxes in the violin plots indicate the pan-cancer samples (n=535) from the LUAD-TCGA cohort and were presented as the median and 25-75th percentile. MDIG, mineral dust-induced gene; HExp, high MDIG expression; LExp, low MDIG expression; LUAD, lung adenocarcinoma; TCGA, The Cancer Genome Atlas.

analysis, MDIG was indicated to be related to biological processes such as RNA splicing, ribonucleoprotein complex biogenesis and carbon metabolism. Furthermore, although the expression of MDIG was not high in normal lung tissue, it was highest in lung cancer cell lines. These results suggested that MDIG may have an important role in the development of lung cancer. Thus, studying the expression of MDIG in cancer cell lines may help guide further cell experimental studies on the regulation of gene expression in the future. In addition, most of the cancer types examined in the present study, including BLCA, CHOL, COAD, ESCA, GBM, LIHC, LUAD, LUSC, PRAD, READ and STAD, exhibited higher MDIG expression than para-cancerous normal tissue. These results suggested that MDIG may be used as a diagnostic marker for these tumors. By contrast, MDIG expression was significantly downregulated in BRCA, KIRC, KIRP, and THCA. This result was the opposite of findings from previous studies with small clinical samples (13,17,49). This may be because of a bias due to the different samples and sample sizes, which requires to be verified by more clinical studies. However, there was no study on the expression of MDIG in patients with THCA.

As previously reported, MDIG expression may be associated with smoking and the expression of MDIG was significantly higher in lung cancer patients who smoked compared with that in non-smokers (50). Since smoking is closely associated with lung cancer, the results using large samples of data from a public database verified that the expression of MDIG in patients with LUAD who smoked was significantly higher than that in patients who did not smoke, suggesting that smoking may lead to high MDIG expression in LUAD. According to the uniCox analysis and KM curves for OS and PFI, high expression of MDIG was significantly associated with poor prognosis in KIRP, LGG, LIHC, PAAD, PRAD, SARC, BLCA, BRCA and UCEC. The present results just confirmed the previous results of clinical studies indicating that high expression of MDIG was significantly associated with poor prognosis of KIRP (49), LIHC (14), PAAD (51) and BRCA (13). At present, there is no literature report on the relationship between MDIG expression and prognosis of LGG,

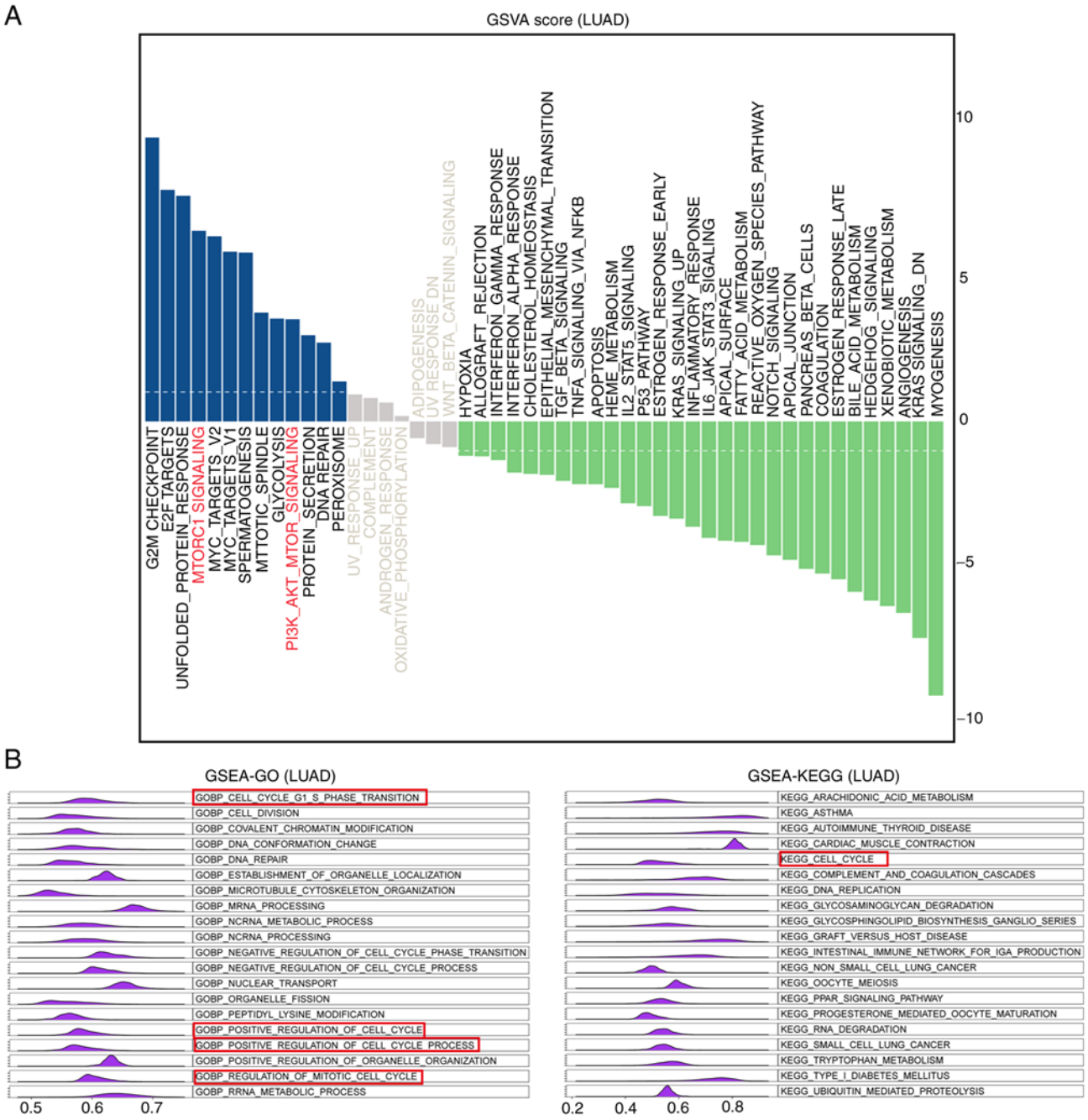

Figure 10. GSVA and GSEA in LUAD. (A) Functional enrichment analysis using GSVA. The y-axis indicates the t-value of the GSVA score. (B) The top 20 GSEA results for GOBP terms and KEGG pathways in LUAD are presented. The x-axis indicates the enrichment score. GSVA, gene set variation analysis; GSEA, gene set enrichment analysis; GOBP, Gene Ontology Biological Process; KEGG, Kyoto Encyclopedia of Genes and Genomes; LUAD, lung adenocarcinoma.

BLCA, SARC and UCEC. In summary, MDIG was not only upregulated in multiple tumor types but also associated with prognosis, suggesting that MDIG may represent a biomarker and prognostic indicator for certain types of tumor.

The results of the present pan-cancer analysis confirmed that MDIG was highly expressed in a variety of tumor types. Furthermore, the possible reasons for the increased expression of MDIG in tumor tissue were examined. The results suggested that 'Amplification' was the main type of MDIG genetic alteration in different types of cancer. Therefore, it may be hypothesized that MDIG amplification may explain the high expression of this gene in a variety of tumor tissues. DNA methylation is one of the most studied epigenetic modifications in mammals. In tumor cells, DNA demethylation was able to promote the expression of certain oncogenes (52). For the first time, the changes in MDIG promoter methylation levels in tumors were explained. As MDIG was abnormally highly expressed in NSCLC, as expected, the promoter methylation levels of MDIG were significantly reduced in LUAD and LUSC. This suggested that hypomethylation of the promoter region of MDIG may be another reason for the high expression of MDIG in tumor tissues. Previous studies have indicated that high expression of MDIG was associated with poor prognosis of patients in the early stage of NSCLC but improved

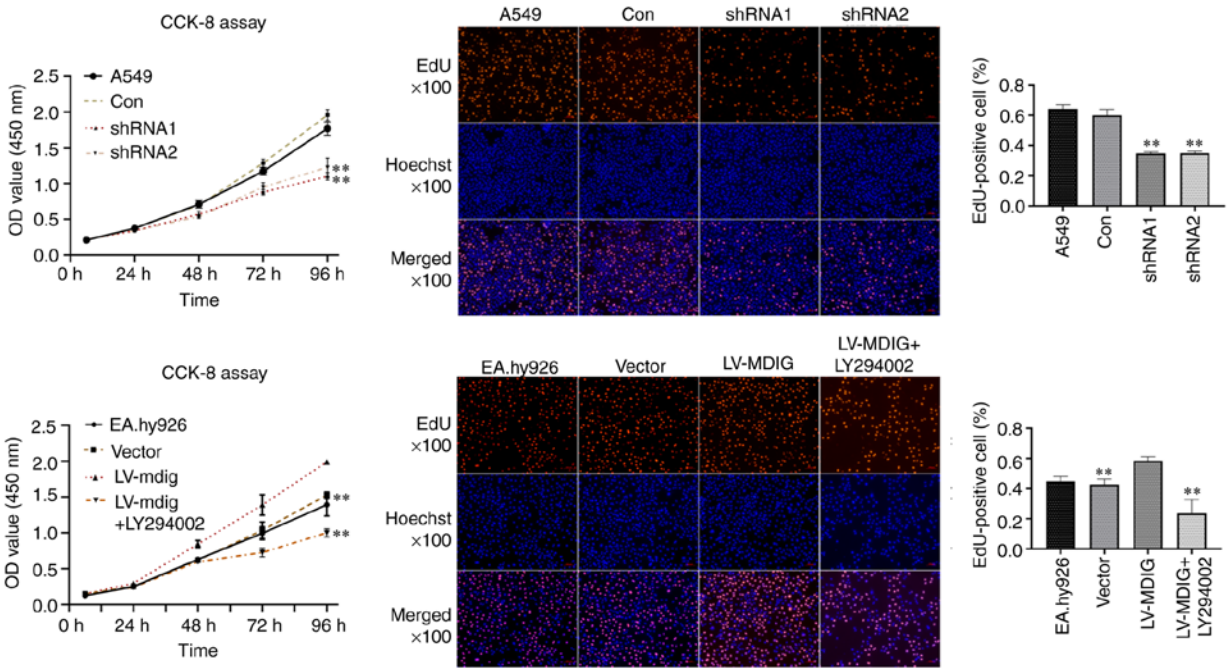

Figure 11. Effect of MDIG on A549 and EA.hy926 cell proliferation. CCK-8 and EdU assays were performed using A549 cells transfected with MDIG-targeting shRNA1 and shRNA2 (top). CCK-8 and EdU assays were carried out in EA.hy926 cells transfected with LV-MDIG and treated with LY294002 (bottom) (magnification, x100). **P<0.01 vs. Con or LV-MDIG group, one-way ANOVA followed by Tukey's post-hoc test. MDIG, mineral dust-induced gene; Con, control; LV, lentiviral vector; shRNA, short hairpin RNA; CCK-8, Cell Counting Kit-8; OD, optical density.

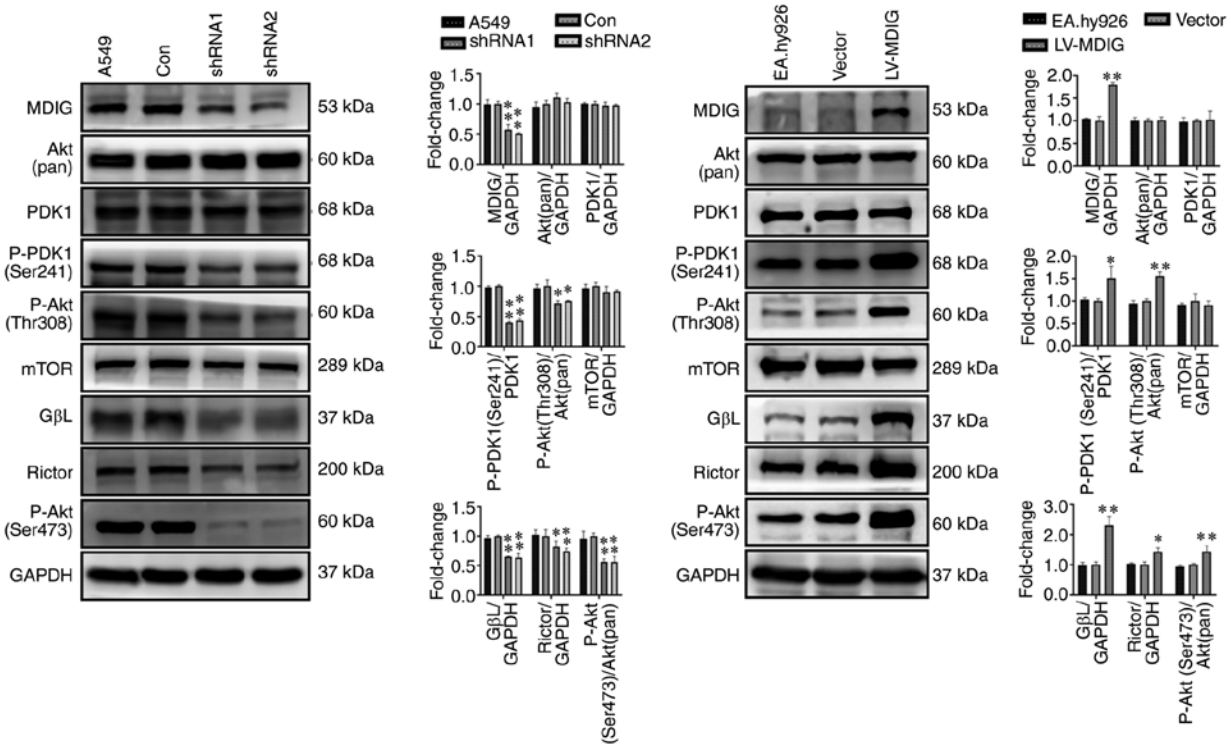

Figure 12. Regulation of the mTORC2/Akt and PDK1/Akt signaling pathway by MDIG. Western blot analysis was used to examine the mTORC2/Akt and PDK1/Akt signaling pathways. GAPDH was used as the loading control. Phosphoproteins were presented as the ratio of phosphoprotein to total protein. *P<0.05, **P<0.01 vs. Con or Vector group (one-way ANOVA followed by Tukey's post-hoc test). MDIG, mineral dust-induced gene; Con, control; LV, lentiviral vector; shRNA, short hairpin RNA; P, phosphorylated; PDK1, pyruvate dehydrogenase kinase 1; mTORC2, mTOR complex 2.

prognosis in the late stage (22). Therefore, LUAD was selected to study the correlation between MDIG expression and that of C-Myc or TP53. MDIG expression was positively correlated with that of C-Myc at stage II/III; it was previously reported that MDIG was a novel target gene of C-Myc and that the gene expression from the MDIG promoter was elevated by c-Myc

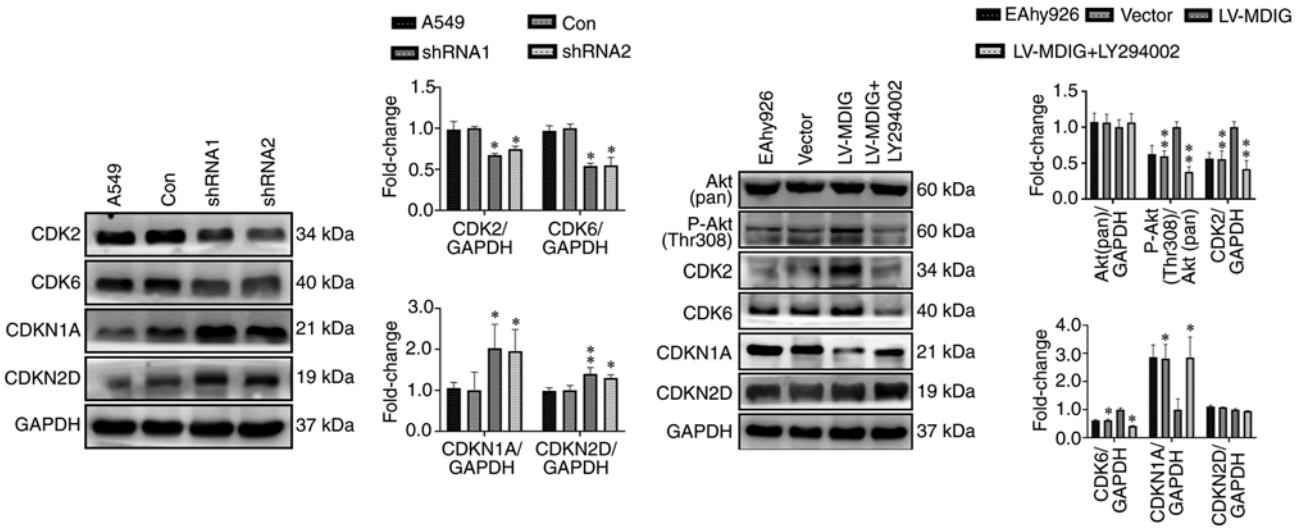

Figure 13. Regulation of the expression of cell cycle-associated proteins by MDIG. Western blot analysis was used to determine the expression levels of cell cycle-associated proteins. GAPDH was used as the loading control. Phosphoprotein was presented as the ratio of phosphoprotein to total protein. *P<0.05, **P<0.01 vs. Con or LV-MDIG group (one-way ANOVA followed by Tukey's post-hoc test). MDIG, mineral dust-induced gene; Con, control; LV, lentiviral vector; shRNA, short hairpin RNA; P, phosphorylated; CDK, cyclin-dependent kinase; CDKN1A, CDK inhibitor 1A.

through E-box sites (6), yet this correlation weakened and was no longer statistically significant at stage IV in the present study. These results indicated that MDIG may be the downstream target gene of C-Myc, but MDIG may not be regulated solely by C-Myc and there may be other transcription factors that may regulate its expression. In addition, the correlation between MDIG and TP53 was weak and insignificant at stage I/II/III, but positive at stage IV. This suggests that MDIG may inhibit tumor progression by promoting the expression of certain tumor suppressor genes in patients with advanced LUAD. However, the underlying molecular mechanisms of these relationships require to be confirmed.

The TME has been widely implicated in tumorigenesis, as it harbors tumor cells that interact with surrounding cells through the circulatory and lymphatic systems to modulate the development and progression of cancer. In addition to malignant cells, adipocytes, fibroblasts, tumor vasculature, lymphocytes, dendritic cells and cancer-associated fibroblasts are also present in the TME (53). Each of these cell types has unique immunological functions that determine whether the tumor will survive and affect neighboring cells (53). Previous reports have demonstrated that MDIG was associated with a variety of human diseases through immune regulation, such as pulmonary fibrosis (5), asthma (54) and nematode expulsion (55). However, there were no studies on the association of MDIG with tumor immunity. In the present study, MDIG expression positively correlated with immune cell infiltration in most types of tumors. However, the correlation of MDIG expression with the infiltration of 'T cells CD8^{+}', 'NK cells activated' and 'Tregs' was negative. Since activated CD8^{+} T cells and NK-cell infiltration predicts favorable prognosis of patients with cancer (53), such as those with gastric cancer (56) and malignant pleural mesothelioma (57), MDIG may lead to a poor prognosis by inhibiting their infiltration in the TME. The negative correlation between MDIG and Treg infiltration was also consistent with previous research, in which immunohistochemistry using the Treg cell marker forkhead box p3 revealed an increased presence of Tregs in the lung of the MDIG$^{+/-}$ mice in response to silica (5). Thus, the expression of MDIG is closely related to immune cell infiltration, suggesting that MDIG has an important role in the TME and may influence the occurrence and development of a tumor by influencing the type and number of infiltrating cells.

The clinical development of checkpoint inhibitor-based immunotherapy has ushered in a promising era for cancer treatment. Durable anti-PD-L1 immune checkpoint blockade responses may be seen in patients with melanoma, LUAD, BLCA and other malignancies (58). By increasing the activity of the immune system, immune checkpoint blockade may have inflammatory side effects, termed immune-related adverse events. The development of predictive biomarkers is required in order to optimize the patient benefit, minimize the risk of toxicities and guide combination treatment approaches (59,60). In the present study, MDIG positively correlated with the frequency of certain tumor-infiltrating immune cells, TME-relevant signatures, immunostimulatory genes, immune checkpoint genes and chemokine receptor genes in most types of tumor except for KIRC and THCA. Furthermore, there was a significant positive correlation between the expression of MDIG and that of PD-L1 in multiple tumor types. Based on these results, it may be hypothesized that MDIG may be a positive immunotherapy biomarker in several tumor types. In addition, MDIG expression also correlated with TMB and MSI in different types of cancer. Therefore, MDIG may be a good prognostic biomarker for LUAD, BLCA, THYM, STAD, UCEC and LUSC in immune checkpoint blockade therapy, but a poor prognostic biomarker for KIRC and THCA. To test this hypothesis, a cohort of patients who had received immunotherapy was used. The results demonstrated that patients with BLCA and high MDIG expression had longer OS after receiving PD-L1 treatment. This result suggested that high expression of MDIG in BLCA may be used as a biomarker for the clinical benefit of patients with cancer after receiving PD-L1 treatment. However, further clinical and molecular

biology studies are required to confirm this finding in different types of cancer in the future.

Furthermore, high expression of MDIG led to multiple drug resistance in the TCGA-LUAD cohort, consistent with previous findings by our group that high expression of MDIG leads to cisplatin resistance in A549 cells, in which MDIG promotes cisplatin resistance of LUAD by regulating ABC transporter expression via activation of the WNT/β-catenin signaling pathway (24). More recently, MDIG-specific small molecule inhibitors, 2-(aryl) alkylthio-3,4-dihydro-4-oxoypyrimidine-5-carboxylic acids, were reported to bind to MDIG through direct interaction with iron cofactors (61). They not only had anti-proliferative activity against cancer cells but also sensitized cancer cells to conventional chemotherapy. In addition, the anti-tumor effect of doxorubicin combined with MDIG inhibitor was synergistic (61). Thus, combination of MDIG inhibitors with existing chemotherapy, targeted therapy and immunotherapy drugs may provide novel effective methods for the treatment of multiple cancer types in the future.

The results of the present enrichment analysis indicated that MDIG was related to the Akt signaling pathway and cell proliferation. In addition, *in vitro* experiments confirmed that MDIG modulated the expression of cycle-related proteins (CDK2, CDK6, CDKN1A and CDKN2D) and promoted cell proliferation through the mTORC2/Akt and PDK1/Akt signaling pathways. In the mTORC2/Akt pathway, MDIG primarily promoted GβL and Rictor expression, which may in turn activate Akt through phosphorylation at Ser473, without affecting mTOR expression. Furthermore, MDIG promoted phosphorylation of PDK1 at Ser241 and also the phosphorylation of Akt at Thr308, without affecting PDK1 expression. In addition, PDK1/Akt inhibitors were used to verify this molecular mechanism.

Although the present study comprehensively analyzed the landscape of MDIG expression in different types of cancer, there were several limitations. First, most of the data were mined using public databases and most of them were results of RNA-seq data. Furthermore, the absence of specific names of the tumor cell lines from the CCLE database was another limitation. In addition, as lung cancer is by far the most common malignancy, the mechanisms of MDIG were primarily explored in LUAD. Finally, *in vitro* experiments were only performed to verify the effect of MDIG on cell proliferation at the protein level, which was because signaling pathway proteins were primarily regulated by post-transcriptional modifications. However, the present study not only revealed the roles of MDIG in different types of cancer but may also guide future research on MDIG in various tumor types. Therefore, more detailed and in-depth studies are required in the future to clarify the significance of MDIG in different types of cancer.

Acknowledgements

Not applicable.

Funding

This work was funded by the Project of Liaoning Distinguished Professor [grant no. (2013) 204 to HZ] and the China Postdoctoral Foundation Project (grant no. 2020M670097ZX to FG).

Availability of data and materials

The datasets used and/or analyzed during the current study are available from the corresponding author on reasonable request. The patient data used are available from the GTEx, CCLE, TCGA and IMvigor210 public databases.

Authors' contributions

FG and HZ contributed to the experimental design. FG, WY, DS and HH collected and analyzed the raw data. FG, BH, HZ and YC performed data analysis. FG participated in the writing of the manuscript and data interpretation. FG and WY conducted the transfection experiments. FG and HZ checked and approved the authenticity of the raw data. All authors read and approved the final manuscript.

Ethics approval and consent to participate

Not applicable.

Patient consent for publication

Not applicable.

Competing interests

The authors declare that they have no competing interests.

References

1. Sung H, Ferlay J, Siegel RL, Laversanne M, Soerjomataram I, Jemal A and Bray F: Global cancer statistics 2020: GLOBOCAN estimates of incidence and mortality worldwide for 36 Cancers in 185 Countries. CA Cancer J Clin 71: 209-249, 2021.
2. Wu K, Li L, Thakur C, Lu Y, Zhang X, Yi Z and Chen F: Proteomic characterization of the world trade center dust-activated mdig and c-myc signaling circuit linked to multiple myeloma. Sci Rep 6: 36305, 2016.
3. Zhang Y, Lu Y, Yuan BZ, Castranova V, Shi X, Stauffer JL, Demers LM and Chen F: The Human mineral dust-induced gene, mdig, is a cell growth regulating gene associated with lung cancer. Oncogene 24: 4873-4882, 2005.
4. Sun J, Yu M, Lu Y, Thakur C, Chen B, Qiu P, Zhao H and Chen F: Carcinogenic metalloid arsenic induces expression of mdig oncogene through JNK and STAT3 activation. Cancer Lett 346: 257-263, 2014.
5. Thakur C, Wolfarth M, Sun J, Zhang Y, Lu Y, Battelli L, Porter DW and Chen F: Oncoprotein mdig contributes to silica-induced pulmonary fibrosis by altering balance between Th17 and Treg T cells. Oncotarget 6: 3722-3736, 2015.
6. Tsuneoka M, Koda Y, Soejima M, Teye K and Kimura H: A novel myc target gene, mina53, that is involved in cell proliferation. J Biol Chem 277: 35450-35459, 2002.
7. Eilbracht J, Kneissel S, Hofmann A and Schmidt-Zachmann MS: Protein NO52-a constitutive nucleolar component sharing high sequence homologies to protein NO66. Eur J Cell Biol 84: 279-294, 2005.
8. Chowdhury R, Sekirnik R, Brissett NC, Krojer T, Ho CH, Ng SG, Clifton LJ, Ge W, Kershaw NJ, Fox GC, *et al*: Ribosomal oxygenases are structurally conserved from prokaryotes to humans. Nature 510: 422-426, 2014.
9. Aziz N, Hong YH, Jo M, Kim JK, Kim KH, Ashktorab H, Smoot DT, Hur H, Yoo BC and Cho AJY: Molecular signatures of JMJD10/MINA53 in gastric cancer. Cancers 12: 1141, 2020.

10. Ge W, Wolf A, Feng T, Ho CH, Sekirnik R, Zayer A, Granatino N, Cockman ME, Loenarz C, Loik ND, *et al*: Oxygenase-catalyzed ribosome hydroxylation occurs in prokaryotes and humans. Nat Chem Biol 8: 960-962, 2012.
11. Zhang Q, Thakur C, Shi J, Sun J, Fu Y, Stemmer P and Chen F: New discoveries of mdig in the epigenetic regulation of cancers. Semin Cancer Biol 57: 27-35, 2019.
12. Komiya K, Sueoka-Aragane N, Sato A, Hisatomi T, Sakuragi T, Mitsuoka M, Sato T, Hayashi S, Izumi H, Tsuneoka M and Sueoka E: Mina53, a novel c-Myc target gene, is frequently expressed in lung cancers and exerts oncogenic property in NIH/3T3 cells. J Cancer Res Clin Oncol 136: 465-473, 2010.
13. Thakur C, Lu Y, Sun J, Yu M, Chen B and Chen F: Increased expression of mdig predicts poorer survival of the breast cancer patients. Gene 535: 218-224, 2014.
14. Zhang L, Huo Q, Ge C, Zhao F, Zhou Q, Chen X, Tian H, Chen T, Xie H, Cui Y, *et al*: ZNF143-mediated H3K9 trimethylation upregulates CDC6 by activating MDIG in hepatocellular carcinoma. Cancer Res 80: 2599-2611, 2020.
15. Teye K, Tsuneoka M, Arima N, Koda Y, Nakamura Y, Ueta Y, Shirouzu K and Kimura H: Increased expression of a Myc target gene Mina53 in human colon cancer. Am J Pathol 164: 205-216, 2004.
16. Xing J, Wang K, Liu PW, Miao Q and Chen XY: Mina53, a novel molecular marker for the diagnosis and prognosis of gastric adenocarcinoma. Oncol Rep 31: 634-640, 2014.
17. Bellut J, Bertz S, Nolte E, Stöhr C, Polifka I, Lieb V, Herrmann E, Jung R, Hartmann A, Wullich B, *et al*: Differential prognostic value of MYC immunohistochemistry in subtypes of papillary renal cell carcinoma. Sci Rep 7: 16424, 2017.
18. Kuratomi K, Yano H, Tsuneoka M, Sakamoto K, Kusukawa J and Kojiro M: Immunohistochemical expression of Mina53 and Ki67 proteins in human primary gingival squamous cell carcinoma. Kurume Med J 53: 71-78, 2006.
19. Teye K, Arima N, Nakamura Y, Sakamoto K, Sueoka E, Kimura H and Tsuneoka M: Expression of myc target gene mina53 in subtypes of human lymphoma. Oncol Rep 18: 841-848, 2007.
20. Thakur C and Chen F: Current understanding of mdig/MINA in human cancers. Genes Cancer 6: 288-302, 2015.
21. Komiya K, Sueoka-Aragane N, Sato A, Hisatomi T, Sakuragi T, Mitsuoka M, Sato T, Hayashi S, Izumi H, Tsuneoka M and Sueoka E: Expression of Mina53, a novel c-Myc target gene, is a favorable prognostic marker in early stage lung cancer. Lung Cancer 69: 232-238, 2010.
22. Yu M, Sun J, Thakur C, Chen B, Lu Y, Zhao H and Chen F: Paradoxical roles of mineral dust induced gene on cell proliferation and migration/invasion. PLoS One 9: e87998, 2014.
23. Thakur C, Chen B, Li L, Zhang Q, Yang ZQ and Chen F: Loss of mdig expression enhances DNA and histone methylation and metastasis of aggressive breast cancer. Signal Transduct Target Ther 3: 25, 2018.
24. Wang Q, Geng F, Zhou H, Chen Y, Du Y, Zhang X, Song D and Zhao H: MDIG promotes cisplatin resistance of lung adenocarcinoma by regulating ABC transporter expression via activation of the WNT/β-catenin signaling pathway. Oncol Lett 18: 4294-4307, 2019.
25. Xuan F, Huang M, Zhao E and Cui H: MINA53 deficiency leads to glioblastoma cell apoptosis via inducing DNA replication stress and diminishing DNA damage response. Cell Death Dis 9: 1062, 2018.
26. Zhou H, Geng F, Chen Y, Du J, Zhang X, Liu B, Song D, Hou H and Zhao H: The mineral dust-induced gene, mdig, regulates angiogenesis and lymphangiogenesis in lung adenocarcinoma by modulating the expression of VEGF-A/C/D via EGFR and HIF-1α signaling. Oncol Rep 45: 60, 2021.
27. GTEx Consortium: The genotype-tissue expression (GTEx) project. Nat Gen 45: 580-585, 2013.
28. The TCGA Legacy. Cell 173: 281-282, 2018.
29. Wang S, Xiong Y, Zhao L, Gu K, Li Y, Zhao F, Li J, Wang M, Wang H, Tao Z, *et al*: UCSCXenaShiny: An R/CRAN Package for interactive analysis of UCSC xena data. Bioinformatics 38: 527-529, 2021.
30. Gao J, Aksoy BA, Dogrusoz U, Dresdner G, Gross B, Sumer SO, Sun Y, Jacobsen A, Sinha R, Larsson E, *et al*: Integrative analysis of complex cancer genomics and clinical profiles using the cBioPortal. Sci Signal 6: pl1, 2013.
31. Chandrashekar DS, Bashel B, Balasubramanya SAH, Creighton CJ, Ponce-Rodriguez I, Chakravarthi BVSK and Varambally S: UALCAN: A portal for facilitating tumor subgroup gene expression and survival analyses. Neoplasia 19: 649-658, 2017.
32. Massó-Vallés D, Beaulieu ME and Soucek L: MYC, MYCL, and MYCN as therapeutic targets in lung cancer. Expert Opin Ther Targets 24: 101-114, 2020.
33. Huang CL, Yokomise H and Miyatake A: Clinical significance of the p53 pathway and associated gene therapy in non-small cell lung cancers. Future Oncol 3: 83-93, 2007.
34. Chen B, Khodadoust MS, Liu CL, Newman AM and Alizadeh AA: Profiling tumor infiltrating immune cells with CIBERSORT. Methods Mol Biol 1711: 243-259, 2018.
35. Ju M, Jiang L, Wei Q, Yu L, Chen L, Wang Y, Hu B, Qian P, Zhang M, Zhou C, *et al*: A immune-related signature associated with TME can serve as a potential biomarker for survival and sorafenib resistance in liver cancer. Onco Targets Ther 14: 5065-5083, 2021.
36. Zeng D, Li M, Zhou R, Zhang J, Sun H, Shi M, Bin J, Liao Y, Rao J and Liao W: Tumor microenvironment characterization in gastric cancer identifies prognostic and immunotherapeutically relevant gene signatures. Cancer Immunol Res 7: 737-750, 2019.
37. Meyers DE and Banerji S: Biomarkers of immune checkpoint inhibitor efficacy in cancer. Curr Oncol 27 (Suppl 2): S106-S114, 2020.
38. Ru B, Wong CN, Tong Y, Zhong JY, Zhong SSW, Wu WC, Chu KC, Wong CY, Lau CY, Chen I, *et al*: TISIDB: An integrated repository portal for tumor-immune system interactions. Bioinformatics 35: 4200-4202, 2019.
39. Mariathasan S, Turley SJ, Nickles D, Castiglioni A, Yuen K, Wang Y, Kadel EE III, Koeppen H, Astarita JL, Cubas R, *et al*: TGFβ attenuates tumour response to PD-L1 blockade by contributing to exclusion of T cells. Nat 554: 544-548, 2018.
40. Yang W, Soares J, Greninger P, Edelman EJ, Lightfoot H, Forbes S, Bindal N, Beare D, Smith JA, Thompson IR, *et al*: Genomics of drug sensitivity in cancer (GDSC): A resource for therapeutic biomarker discovery in cancer cells. Nucleic Acids Res 41: D955-D961, 2013.
41. Geeleher P, Cox N and Huang RS: pRRophetic: An R package for prediction of clinical chemotherapeutic response from tumor gene expression levels. PLoS One 9: e107468, 2014.
42. Geeleher P, Cox NJ and Huang RS: Clinical drug response can be predicted using baseline gene expression levels and in vitro drug sensitivity in cell lines. Genome Biol 15: R47, 2014.
43. Hänzelmann S, Castelo R and Guinney J: GSVA: Gene set variation analysis for microarray and RNA-seq data. BMC Bioinformatics 14: 7, 2013.
44. Powers RK, Goodspeed A, Pielke-Lombardo H, Tan AC and Costello JC: GSEA-InContext: Identifying novel and common patterns in expression experiments. Bioinformatics 34: i555-i564, 2018.
45. Choucair K, Morand S, Stanbery L, Edelman G, Dworkin L and Nemunaitis J: TMB: A promising immune-response biomarker, and potential spearhead in advancing targeted therapy trials. Cancer Gene Ther 27: 841-853, 2020.
46. Bouchez C, Kempf E and Tournigand C: MSI Metastatic solid tumors treatment and immunotherapies. Bull Cancer 106: 143-150, 2019.
47. Kaur J, Elms J, Munn AL, Good D and Wei MQ: Immunotherapy for non-small cell lung cancer (NSCLC), as a stand-alone and in combination therapy. Crit Rev Oncol Hematol 164: 103417, 2021.
48. Yu JS and Cui W: Proliferation, survival and metabolism: The role of PI3K/AKT/mTOR signalling in pluripotency and cell fate determination. Development 143: 3050-3060, 2016.
49. Ferreira MJ, Pires-Luís AS, Vieira-Coimbra M, Costa-Pinheiro P, Antunes L, Dias PC, Lobo F, Oliveira J, Gonçalves CS, Costa BM, *et al*: SETDB2 and RIOX2 are differentially expressed among renal cell tumor subtypes, associating with prognosis and metastization. Epigenetics 12: 1057-1064, 2017.
50. Shi J, Thakur C, Zhao Y, Li Y, Nie L, Zhang Q, Bi Z, Fu Y, Wadgaonkar P, Almutairy B, *et al*: Pathological and prognostic indications of the mdig gene in human lung cancer. Cell Physiol Biochem 55: 13-28, 2021.
51. Tan XP, Dong WG, Zhang Q, Yang ZR, Lei XF and Ai MH: Potential effects of Mina53 on tumor growth in human pancreatic cancer. Cell Biochem Biophys 69: 619-625, 2014.
52. Kulis M and Esteller M: DNA methylation and cancer. Adv Genet 70: 27-56, 2010.
53. Arneth B: Tumor microenvironment. Medicina (Kaunas) 56: 15, 2019.
54. Mori T, Okamoto K, Tanaka Y, Teye K, Umata T, Ohneda K, Tokuyama K, Okabe M and Tsuneoka M: Ablation of Mina53 in mice reduces allergic response in the airways. Cell Struct Funct 38: 155-167, 2013.

55. Pillai MR, Mihi B, Ishiwata K, Nakamura K, Sakuragi N, Finkelstein DB, McGargill MA, Nakayama T, Ayabe T, Coleman ML and Bix M: Myc-induced nuclear antigen constrains a latent intestinal epithelial cell-intrinsic anthelmintic pathway. PLoS One 14: e0211244, 2019.
56. Chen T, Yang C, Dou R and Xiong B: Identification of a novel 10 immune-related genes signature as a prognostic biomarker panel for gastric cancer. Cancer Med 10: 6546-6560, 2021.
57. Yamada N, Oizumi S, Kikuchi E, Shinagawa N, Konishi-Sakakibara J, Ishimine A, Aoe K, Gemba K, Kishimoto T, Torigoe T and Nishimura M: CD8+ tumor-infiltrating lymphocytes predict favorable prognosis in malignant pleural mesothelioma after resection. Cancer Immunol Immunother 59: 1543-1549, 2010.
58. Pilard C, Ancion M, Delvenne P, Jerusalem G, Hubert P and Herfs M: Cancer immunotherapy: It's time to better predict patients' response. Br J Cancer 125: 927-938, 2021.
59. Postow MA, Sidlow R and Hellmann MD: Immune-related adverse events associated with immune checkpoint blockade. N Engl J Med 378: 158-168, 2018.
60. Gibney GT, Weiner LM and Atkins MB: Predictive biomarkers for checkpoint inhibitor-based immunotherapy. Lancet Oncol 17: e542-e551, 2016.
61. Nowak RP, Tumber A, Hendrix E, Ansari MSZ, Sabatino M, Antonini L, Andrijes R, Salah E, Mautone N, Pellegrini FR, *et al*: First-in-class inhibitors of the ribosomal oxygenase MINA53. J Med Chem 64: 17031-17050, 2021.